

NUMERICAL ESTIMATION OF COERCIVITY CONSTANTS FOR BOUNDARY INTEGRAL OPERATORS IN ACOUSTIC SCATTERING*

T. BETCKE[†] AND E. A. SPENCE[‡]

Abstract. Coercivity is an important concept for proving existence and uniqueness of solutions to variational problems in Hilbert spaces. But while coercivity estimates are well known for many variational problems arising from partial differential equations, they are still an open problem in the context of boundary integral operators arising from acoustic scattering problems, where rigorous coercivity results have so far only been established for combined integral operators on the unit circle and sphere. The fact that coercivity holds, even in these special cases, is perhaps surprising, as formulations of Helmholtz problems are generally thought to be indefinite. The main motivation for investigating coercivity in this context is that it has the potential to give error estimates for the Galerkin method which are both explicit in the wavenumber k and valid regardless of the approximation space used; thus they apply to hybrid asymptotic-numerical methods recently developed for the high frequency case. One way to interpret coercivity is by considering the numerical range of the operator. The numerical range is a well established tool in spectral theory, and algorithms exist to approximate the numerical range of finite dimensional matrices. We can, therefore, use Galerkin projections of the boundary integral operators to approximate the numerical range of the original operator. We prove convergence estimates for the numerical range of Galerkin projections of a general bounded linear operator on a Hilbert space to justify this approach. By computing the numerical range of the combined integral operator in acoustic scattering for several interesting convex, nonconvex, smooth, and polygonal domains, we numerically study coercivity estimates for varying wavenumbers. We find that coercivity holds, uniformly in the wavenumber k , for a wide variety of domains. Finally, we consider a trapping domain, for which there exist resonances (also called scattering poles) very close to the real line, to demonstrate that coercivity for a certain wavenumber k seems to be strongly dependent on the distance to the nearest resonance.

Key words. numerical range, coercivity, boundary integral operators, high frequency, resonance

AMS subject classifications. 45P05, 47A12, 65R20

DOI. 10.1137/100788483

1. Introduction. Let \mathcal{H} be a Hilbert space, and let $t : \mathcal{H} \times \mathcal{H} \rightarrow \mathbb{C}$ be a sesquilinear form on \mathcal{H} . A standard variational problem is to find $u \in \mathcal{H}$ such that

$$(1.1) \quad t(u, v) = f(v) \quad \forall v \in \mathcal{H}$$

for a given $f \in \mathcal{H}'$, the dual space of \mathcal{H} . It is a classical result that there exists a unique solution to this problem if there exist $C, \gamma > 0$ such that

$$(1.2) \quad |t(u, v)| \leq C \|u\| \|v\| \quad \forall u, v \in \mathcal{H} \text{ (continuity),}$$

$$(1.3) \quad \gamma \|u\|^2 \leq |t(u, u)| \quad \forall u \in \mathcal{H} \text{ (coercivity).}$$

*Received by the editors March 12, 2010; accepted for publication (in revised form) April 22, 2011; published electronically August 4, 2011.

<http://www.siam.org/journals/sinum/49-4/78848.html>

[†]Department of Mathematics, University College London, London, WC1E 6BT, UK (t.betcke@ucl.ac.uk). This author's work was supported by Engineering and Physical Sciences Research Council grant EP/H004009/1.

[‡]Department of Mathematics, University of Bath, Bath, BA2 7AY, UK (e.a.spence@bath.ac.uk). This author's work was supported by Engineering and Physical Sciences Research Council grant EP/F06795X/1.

Furthermore, if $u^{(h)}$ is a Galerkin solution of (1.1) in a finite dimensional subspace $\mathcal{V}^{(h)} \subset \mathcal{H}$, then C ea’s lemma [8] gives

$$(1.4) \quad \|u - u^{(h)}\| \leq \frac{C}{\gamma} \inf_{v \in \mathcal{V}^{(h)}} \|u - v\|.$$

Hence, the stability of the Galerkin approximation $u^{(h)}$ can be determined by the continuity constant C and the coercivity constant γ .

While estimates for γ are known for variational formulations of several classical PDEs they are still an open problem for boundary integral operators in acoustic scattering. Consider the problem of time-harmonic acoustic scattering from a sound-soft bounded obstacle $\Omega \subset \mathbb{R}^d$ ($d = 2, 3$) with Lipschitz boundary $\Gamma := \partial\Omega$. That is, we are looking for the solution u of the problem

$$(1.5) \quad \Delta u + k^2 u = 0 \quad \text{in } \mathbb{R}^d \setminus \overline{\Omega},$$

$$(1.6) \quad u = 0 \quad \text{on } \Gamma,$$

$$(1.7) \quad \frac{\partial u_s}{\partial r} - ik u_s = o(r^{-(d-1)/2}),$$

where $u = u_{inc} + u_s$ is the total field, u_{inc} is an entire solution of (1.5), such as an incident plane wave, u_s is the scattered field, r is the radial coordinate, and $k > 0$ is the wavenumber. With the standard free-space Green’s function defined as

$$\Phi(x, y) = \frac{i}{4} H_0^{(1)}(k|x - y|), \quad d = 2, \quad \Phi(x, y) = \frac{e^{ik|x-y|}}{4\pi|x - y|}, \quad d = 3,$$

for $x, y \in \mathbb{R}^d, x \neq y$, the solution u is given by

$$u(x) = u_{inc}(x) - \int_{\Gamma} \Phi(x, y) u_n(y) ds(y), \quad x \in \mathbb{R}^d \setminus \overline{\Omega},$$

where u_n is the outward pointing normal derivative of u . To compute u_n one can solve the boundary integral equation

$$(1.8) \quad A_{k,\eta} u_n = 2 \frac{\partial u_{inc}}{\partial n} - 2i\eta u_{inc}$$

with

$$(1.9) \quad A_{k,\eta} := I + K'_k - i\eta S_k,$$

where $\eta \in \mathbb{R} \setminus \{0\}$, I is the identity, and K'_k and S_k are defined by

$$K'_k u(x) := 2 \int_{\Gamma} \frac{\partial \Phi(x, y)}{\partial n(x)} u(y) ds(y), \quad S_k u(x) := 2 \int_{\Gamma} \Phi(x, y) u(y) ds(y), \quad x \in \Gamma.$$

Here $n(x)$ is the outward pointing unit normal at Γ . Standard trace results imply that the unknown Neumann boundary value u_n is in $H^{-1/2}(\Gamma)$, and a regularity result due to Ne as [34] (quoted in, e.g., [30, Thm. 4.24]) implies that u_n is, in fact, in $L^2(\Gamma)$. Thus we can consider the integral equation (1.8) as an operator equation in $L^2(\Gamma)$, which is a natural space for the practical solution of second kind integral equations since it is self-dual. The corresponding sesquilinear form is defined as

$$a_{k,\eta}(u, v) := \langle A_{k,\eta} u, v \rangle,$$

with $\langle u, v \rangle := \int_{\Gamma} u(y) \overline{v(y)} ds(y)$ being the standard $L^2(\Gamma)$ -inner product. It was recently shown by Chandler-Wilde and Langdon in [13] that the operator $A_{k,\eta}$ is bijective with bounded inverse in the Sobolev spaces $H^{s-1/2}(\Gamma)$ for $|s| \leq \frac{1}{2}$ and $\eta \in \mathbb{R} \setminus \{0\}$ (see also the book by Colton and Kress [15] for the unique solvability of (1.8) in $C(\Gamma)$ with C^2 boundary).

The common choice for the coupling parameter η is to take η proportional to k for k large, and η constant (when $d = 3$) or proportional to $(\log k)^{-1}$ (when $d = 2$) for k small. This has been based on theoretical studies for the case of Γ a circle or sphere [26, 25, 1, 2], and also on computational experience [9]. Recently this choice has been backed up as near optimal for conditioning for more general domains by the analysis of [12] and [5]. In this paper we are interested in the case when k is large, and therefore always choose $\eta = k$. Hence, to simplify notation we will write A and similarly $a(\cdot, \cdot)$ instead of $A_{k,k}$ and $a_{k,k}(\cdot, \cdot)$, unless otherwise stated. However, it is important to keep in mind that A and $a(\cdot, \cdot)$ are k -dependent.

In acoustic scattering, the continuity of $a(\cdot, \cdot)$ is much easier to establish than coercivity. The key question is not only whether $a(\cdot, \cdot)$ is coercive or not, but also how γ (if it exists) depends on the wavenumber k . Indeed, this is the main motivation for studying the variational form of (1.8). The classical theory of second kind integral equations such as (1.8), which is based on the fact that for sufficiently smooth domains the operator (1.9) is a compact perturbation of the identity, gives quasi-optimal error estimates of the form (1.4) when the approximation space $\mathcal{V}^{(h)}$ consists of piecewise polynomials, once the discretization is sufficiently fine. However, these error estimates have the following two disadvantages: The first is that they are not explicit in the wavenumber k , i.e., they do not say how either the constant on the right-hand side of (1.4), or the element size h , depends on k [3, Theorem 3.1.1]. The second is that much research effort has been focused recently on designing novel approximation spaces that take into account the high oscillation of the solution as k increases [11], and it does not appear that the classical theory can be used to prove error estimates for numerical methods using these subspaces. On the other hand, if continuity (1.2) and coercivity (1.3) of $a(\cdot, \cdot)$ can be established with constants C, γ explicit in k , then the error estimate (1.4) is valid for $\mathcal{V}^{(h)}$ any finite dimensional subspace of $L^2(\Gamma)$.

Recently a k -explicit proof of (1.4) for the case when $\mathcal{V}^{(h)}$ consists of piecewise polynomials and when Γ is analytic has been given in [29]. This technique derives stability estimates from approximation results for suitable adjoint problems and relies on a novel splitting of the operator A [31]. However, it does not appear that these methods can be applied to the case when $\mathcal{V}^{(h)}$ is a novel k -dependent approximation space.

A first result on the coercivity of $a(\cdot, \cdot)$ was given in [17], where it was shown that if Γ is the unit circle (in 2-d) or the unit sphere (in 3-d), then $a(\cdot, \cdot)$ is coercive for sufficiently large k with $\gamma \geq 1$. However, the question of coercivity and of k -dependence of γ is still unanswered for more complicated domains. The fact that coercivity *can* hold in this context is perhaps surprising since formulations of Helmholtz problems are usually thought to be indefinite. Indeed, the usual analysis of both domain-based and integral equation-based formulations is to attempt to prove a Gårding inequality, i.e., to attempt to show that the relevant operator is a compact perturbation of a coercive operator. Moreover, in the boundary integral context, for general Lipschitz domains not even a Gårding inequality is known for $a(\cdot, \cdot)$.

The aim of this paper is to investigate the conditions under which coercivity holds, with a particular emphasis on the k -dependence of the coercivity constant γ .

In section 2 we give an overview of existing coercivity results. To numerically estimate the coercivity constant on more complicated domains we use the close connection between coercivity and the numerical range of the operator A . The numerical range is defined as the set of all values $\langle Au, u \rangle$ in the complex plane with $u \in L^2(\Gamma)$, $\|u\| = 1$. It holds that $a(\cdot, \cdot)$ is coercive if and only if 0 is not in the closure of the numerical range. Hence, we can determine coercivity by computing the numerical range of the operator A , which is a well studied problem in the numerical linear algebra literature for matrices acting on \mathbb{C}^n . In section 3 we describe some key properties of the numerical range, and in section 4.1 we review a well known simple algorithm for computing the numerical range of an operator. Since in practice we need to work with Galerkin discretizations of $a(\cdot, \cdot)$, in section 4.2 we give convergence estimates of the numerical range based on Galerkin discretizations with standard piecewise constant boundary element discretizations. In section 5 we demonstrate numerically the convergence of the numerical range and use the numerical range computations to give numerical estimates of the coercivity constant for several interesting polygonal and smooth domains in 2-d. Surprisingly, based on our numerical results coercivity seems to hold independently of the wavenumber on a wide range of interesting domains. We summarize our results and give some conjectures about the coercivity constant in section 6.

2. A summary of stability results for boundary integral operators in acoustic scattering. In this section we summarize the known continuity and coercivity results about the operator A , namely, whether the inequalities (1.2) and (1.3) hold, and if so, how the constants C and γ depend on k . We note that these results also apply to the related operator:

$$(2.1) \quad A'_{k,\eta} := I + K_k - i\eta S_k,$$

where K_k is the double layer potential

$$K_k u(x) := 2 \int_{\Gamma} \frac{\partial \Phi(x, y)}{\partial n(y)} u(y) ds(y), \quad x \in \Gamma.$$

This operator appears in the classic indirect boundary integral formulation due to Brakhage and Werner [7], Leis [28], and Panič [35]. (*Indirect* refers to the fact that this integral operator does not arise from Green’s integral representation, whereas the so-called *direct* integral operator (1.9) does.) The operator $A'_{k,\eta}$ is the adjoint of $A_{k,\eta}$ with respect to the real inner product $\langle u, v \rangle_{\mathbb{R}} := \int_{\Gamma} u(y)v(y)ds(y)$. Thus

$$\|A_{k,\eta}\| = \|A'_{k,\eta}\|,$$

where the norm is that induced by the standard $L^2(\Gamma)$ -inner product, and if the inequalities (1.2), (1.3) hold for $A_{k,\eta}$, then they also hold for $A'_{k,\eta}$ with the same C, γ .

Much less is known about coercivity (1.3) than continuity (1.2), so we discuss coercivity first. We then include a brief discussion of continuity results; for more comprehensive treatments, see [12, 11]. In this section we will use the notation $D \lesssim E$ when D/E is less than a constant which is independent of k .

2.1. Coercivity. The only domains for which coercivity is completely understood are the circle (in 2-d) and sphere (in 3-d); this is because the operator A acts diagonally in the basis of trigonometric polynomials or spherical harmonics in 2-d and 3-d, respectively. For the circle, Domínguez, Graham, and Smyshlyaev [17] showed that, for the case $\eta = k$, coercivity holds for all sufficiently large k with

$$\gamma \geq 1,$$

and for the sphere they proved

$$\gamma \geq 1 - \mathcal{O}(k^{-2/3}).$$

These difficult proofs relied on bounding below the eigenvalues of A , which are combinations of Bessel functions, uniformly in argument and order.

Although nothing is known directly about the coercivity constant γ for domains other than the circle/sphere, results about the norm of the inverse of A can be used to deduce information about γ using the fact that if A is coercive, then

$$\gamma \leq \frac{1}{\|A^{-1}\|}.$$

This follows from (1.3) using Cauchy–Schwarz. Chandler-Wilde et al. [12] proved that if a part of Γ is C^1 , then

$$(2.2) \quad \|A^{-1}\| \geq 1$$

and hence

$$(2.3) \quad \gamma \leq 1.$$

Thus the bound obtained for γ for the circle in [17] is sharp. The inequality (2.2) follows from the fact that S_k and K'_k are smoothing operators on smooth parts of Γ . In the same paper the authors showed that for a particular class of nonconvex, nonstarlike, *trapping* domains in 2-d there exists an increasing sequence k_n such that $\|A^{-1}\|$ grows as k_n increases. Indeed, for these domains, when $\eta = k$,

$$(2.4) \quad \|A^{-1}\| \gtrsim k_n^{9/10}.$$

It is not known whether A is coercive for these domains or not, but this example shows that if it is coercive, it cannot be uniformly coercive in k since

$$\gamma \lesssim k_n^{-9/10},$$

which tends to zero as $k_n \rightarrow \infty$. This result applies to domains with a rectangular cavity; an example of such a domain is given in section 5.3 (see Figure 5.10). Recently it has been proven that for domains with an ellipse-shaped cavity $\|A^{-1}\|$ grows *exponentially* as $k \rightarrow \infty$ through some sequence [5].

The final result on $\|A^{-1}\|$ that is relevant for coercivity was obtained by Chandler-Wilde and Monk in [14]. Their result implies that if Γ is Lipschitz, C^2 in a neighborhood of almost every $x \in \Gamma$, and starlike with respect to the origin, that is,

$$\operatorname{ess\,inf}_{x \in \Gamma} x \cdot n(x) > 0,$$

then for $\eta \gtrsim k$

$$\|A^{-1}\| \lesssim 1.$$

Thus, the blow-up of $\|A^{-1}\|$ for the *trapping* domains in [12], [5] cannot occur when Ω is starlike.

Although proving coercivity of A is still a largely open problem, some progress has been made recently in proving coercivity of a modified boundary integral operator for acoustic scattering. In [37] it was shown that coercivity holds uniformly in k for this modified operator for all star-shaped Lipschitz domains.

2.2. Continuity. By Cauchy–Schwarz, (1.2) holds for the sesquilinear form involving A with $C = \|A\|$, and this is seen to be sharp by letting $v = Au$. The question of bounding $\|A\|$ was investigated in detail in [12]. We summarize the main results below for the case $\eta = k$, noting that [12] obtains bounds explicit in both η and k .

In 2-d and 3-d, for Γ Lipschitz and piecewise C^1 , if k is sufficiently large, then

$$1 \leq \|A\| \lesssim k^{(d-1)/2},$$

where d is the dimension. In 2-d if Γ is piecewise C^2 , there is an improved lower bound leading to

$$(2.5) \quad k^{1/3} \lesssim \|A\| \lesssim k^{1/2}$$

for sufficiently large k . In addition, in 2-d if Γ contains a straight line segment of length a , then

$$(2.6) \quad \|A\| \gtrsim (ak)^{1/2}$$

for sufficiently large k , so that in this case the upper bound (2.5) is sharp in its k -dependence.

For the circle and sphere, the Fourier basis allows for bounds on $\|A\|$ to be obtained by bounding the eigenvalues of A , and this specialized method obtains sharper bounds than the general methods of [12]. For the circle and the sphere, when $\eta = k$ and k is sufficiently large,

$$\|A\| \lesssim k^{1/3}$$

[17]. (This result was obtained earlier for the sphere in the unpublished thesis [20].) Banjai and Sauter [4] recently obtained an improved bound on $\|A\|$ for the sphere: when k is sufficiently large

$$\|A_{k,\eta}\| \lesssim (1 + |\eta|k^{-2/3}).$$

This result, obtained by improved bounds on the eigenvalues, reduces to the earlier bound if $\eta = k$, but becomes independent of k for $\eta = k^{2/3}$.

3. The numerical range and its connections to coercivity. In this section we discuss the connections between the numerical range of a bounded linear operator T on a Hilbert space with associated sesquilinear form $t(u, v) = \langle Tu, v \rangle$ and the coercivity constant γ . From (1.3) it follows that the largest possible coercivity constant γ is determined by

$$(3.1) \quad \gamma = \inf_{u \in \mathcal{H}} \frac{|t(u, u)|}{\|u\|^2}.$$

This value is closely related to the numerical range of T .

DEFINITION 3.1 (numerical range). *Let T be a bounded linear operator in a Hilbert space \mathcal{H} . The numerical range $W(T)$ is defined as the set*

$$W(T) = \{ \langle Tu, u \rangle : u \in \mathcal{H}, \|u\| = 1 \}.$$

The numerical range is also known under the name *field of values*. A beautiful summary of the numerical range and its connections to spectra and pseudospectra is given by Trefethen and Embree in [40]. Many results about the numerical range of linear operators in Hilbert spaces are contained in the book by Gustafson and Rao [22]. The numerical range has the following fundamental properties.

PROPOSITION 3.2 (properties of the numerical range).

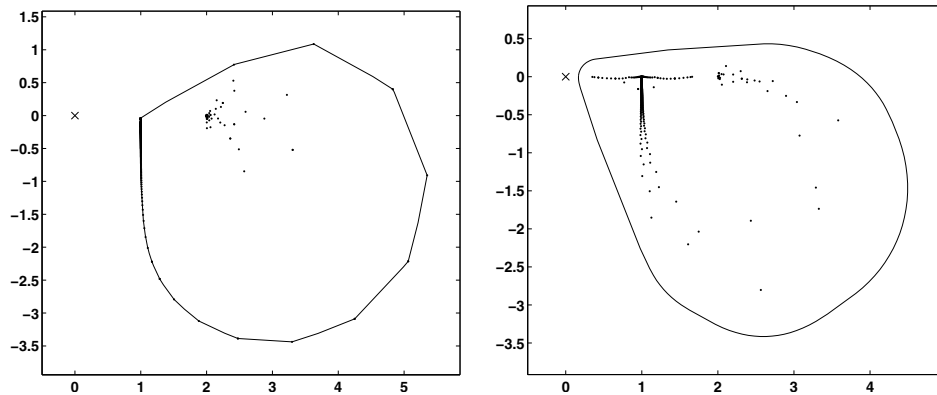


FIG. 3.1. Eigenvalues and boundary of the numerical range of the boundary integral operator A on the unit circle (left plot) and on the equilateral triangle with side length 1 (right plot) for $k = 50$.

1. $W(T)$ is convex.
2. The spectrum $\sigma(T)$ is contained in the closure of $W(T)$.
3. The closure of the numerical range of a normal operator is the convex hull of its spectrum $\sigma(T)$.

The proofs can be found in [22]. From the definition of the numerical range we have the following equivalent characterization of coercivity.

PROPOSITION 3.3. *The sesquilinear form $t(u, v) := \langle Tu, v \rangle$ associated with a bounded linear operator T on a Hilbert space is coercive if and only if $0 \notin \overline{W(T)}$. Furthermore, if $t(\cdot, \cdot)$ is coercive, then the coercivity constant γ is given by $\gamma = \inf_{z \in W(T)} |z|$.*

Proof. If $t(\cdot, \cdot)$ is coercive then, by definition, $0 < \inf_{u \in \mathcal{H} \setminus \{0\}} \frac{|\langle Tu, u \rangle|}{\langle u, u \rangle}$. Hence $0 \notin \overline{W(T)}$. On the other hand, if $t(\cdot, \cdot)$ is not coercive, there exists a sequence $u^{(n)} \subset \mathcal{H} \setminus \{0\}$ such that $\frac{\langle Tu^{(n)}, u^{(n)} \rangle}{\langle u^{(n)}, u^{(n)} \rangle} \rightarrow 0$ for $n \rightarrow \infty$. Therefore, $0 \in \overline{W(T)}$. It follows immediately from (1.3) that $\gamma = \inf_{z \in W(T)} |z|$ if $t(\cdot, \cdot)$ is coercive. \square

This result allows us to rephrase the question of determining coercivity to the question of computing the numerical range $W(T)$. In fact, if T is normal, then we immediately obtain from Proposition 3.2 the following characterization.

PROPOSITION 3.4. *If T is normal, then the associated sesquilinear form $t(\cdot, \cdot)$ is coercive if and only if 0 is not in the closed convex hull of the spectrum of T .*

An example is the operator A defined in (1.9) on the unit circle.

LEMMA 3.5. *If Γ is the boundary of the unit circle (in 2-d) or the unit sphere (in 3-d), then A is normal.*

Proof. On the unit circle the integral operators K' and S and their adjoints diagonalize in the Fourier basis $(e^{in\theta})_{n=-\infty \dots \infty}$. On the unit sphere they diagonalize in the basis of spherical harmonics $(Y_n^m(\hat{x}))_{n \in \mathbb{Z}^+, -n \leq m \leq n}$ [26, 25, 17]. Hence, in both cases A and its adjoint A^* commute. \square

In the left plot of Figure 3.1 the boundary of the numerical range is shown for the operator A on the unit circle with $k = 50$ (we explain how this was computed in section 4.1). The black dots are the eigenvalues of the Galerkin discretization used for this computation. As expected, the numerical range is the convex hull of the eigenvalues. Since on smooth curves Γ the operator A is a compact perturbation of the identity, the point 1 is the limit point of $\sigma(A)$, which is visible in the plot.

Interestingly, some eigenvalues also seem to cluster around 2.

Let us now consider a more interesting domain. In the right plot of Figure 3.1 we show the eigenvalues and the numerical range for the operator A on the boundary of an equilateral triangle with side length 1 and $k = 50$. Two observations are of interest. First of all, the numerical range is again bounded away from zero. Hence, the associated sesquilinear form is coercive for this k . Second, the numerical range is not the convex hull of the eigenvalues anymore. This shows that the corresponding operator A is not normal, and, as a consequence, that spectral information is not sufficient anymore to determine whether the operator is coercive or not.

Characterizations of when $0 \in \overline{W(T)}$ were given by Burke and Greenbaum in [10]. They proved the following equivalence relation.

PROPOSITION 3.6. *Let T be a bounded linear operator. The following statements are equivalent:*

- (i) $0 \notin \overline{W(T)}$.
- (ii) *There exists $c \in \mathbb{C}$ such that $\overline{W(cT)}$ lies in the open right half-plane.*
- (iii) $\min \{ \|I - cT\| : c \in \mathbb{C} \} < 1$.

Statement (ii) is equivalent to the existence of $\alpha > 0$ and $c \in \mathbb{C}$, $|c| = 1$, such that $\operatorname{Re}\langle cTu, u \rangle \geq \alpha$ for all $u \in \mathcal{H}$. This is sometimes used instead of (1.3) as definition of coercivity. Statement (iii) as characterization of coercivity has not been previously encountered by the authors. Its theoretical appeal is that it turns the question of proving coercivity of a bounded linear operator T into the question of estimating the norm of $I - cT$ for constants $c \in \mathbb{C}$.

The numerical range is not only of interest for the estimation of coercivity constants, it tells us much more about an operator. Let $r(T) := \sup\{|z| : z \in W(T)\}$ be the *numerical radius* of T . The numerical radius of T is equivalent to $\|T\|$ since

$$(3.2) \quad r(T) \leq \|T\| \leq 2r(T)$$

(see [22, Theorem 1.3-1]). Both the lower and upper bounds are sharp. This result together with (3.1) allows us to formulate Céa’s lemma (1.4) purely using the numerical range.

THEOREM 3.7 (Céa’s lemma). *Let T be a bounded and coercive linear operator, let $\mathcal{V}^{(h)}$ be a subspace of \mathcal{H} , and let $W(T)$ be the numerical range of T . Then for the Galerkin solution $u^{(h)}$ of (1.1) in the subspace $\mathcal{V}^{(h)}$ we have the estimate*

$$\|u - u^{(h)}\| \leq 2d(T) \inf_{v \in \mathcal{V}^{(h)}} \|u - v\|,$$

where $d(T) := \frac{\sup_{z \in W(T)} |z|}{\inf_{z \in W(T)} |z|}$.

The numerical range is also of practical interest for matrix iterations. For example, bounds for the convergence of GMRES applied to T can be formulated based on the numerical range [18, 19]. Hence, it is justified to study not only the coercivity and continuity constants γ and C separately but to consider the numerical range $W(T)$ itself. In particular, for boundary integral operators in acoustic scattering it is of interest to study the k -dependence of the numerical range, as discussed in section 1.

4. Computing the numerical range. In section 3 we showed that coercivity constants are determined by the distance of the numerical range to the origin. In this section we discuss the approximation of the numerical range. We start with the standard algorithm for computing the numerical range and then give a detailed convergence analysis given that we will be working with finite dimensional Galerkin approximations of the operator.

4.1. An algorithm for numerical range computations. Standard algorithms for computing the numerical range are based on the following principle. Let T be a bounded linear operator on a Hilbert space. We split up T as $T = T_H + iT_S$, where $T_H := \frac{1}{2}(T + T^*)$ and $T_S := \frac{1}{2i}(T - T^*)$; T_H is the self-adjoint (or Hermitian) part of T and iT_S is its skew-adjoint part. Then

$$\frac{\langle Tu, u \rangle}{\langle u, u \rangle} = \frac{\langle T_H u, u \rangle}{\langle u, u \rangle} + i \frac{\langle T_S u, u \rangle}{\langle u, u \rangle}.$$

Since T_H and T_S are self-adjoint, $\langle T_H u, u \rangle \in \mathbb{R}$ and $\langle T_S u, u \rangle \in \mathbb{R}$ for all $u \in \mathcal{H}$. It follows that the real part of every element in the numerical range is determined by T_H . Hence, $W(T)$ is contained in the strip $\{z \in \mathbb{C} : h^{(m)} \leq \operatorname{Re}\{z\} \leq h^{(M)}\}$, where

$$(4.1) \quad h^{(m)} = \inf_{u \in \mathcal{H} \setminus \{0\}} \frac{\langle T_H u, u \rangle}{\langle u, u \rangle}, \quad h^{(M)} = \sup_{u \in \mathcal{H} \setminus \{0\}} \frac{\langle T_H u, u \rangle}{\langle u, u \rangle}.$$

By multiplying the operator T with $e^{i\theta}$ for $\theta \in [0, \pi]$ and computing $h^{(m)}$ and $h^{(M)}$ again we obtain a set of enclosing lines that characterize the convex set $W(T)$. Denote by $h_\theta^{(m)}$ and $h_\theta^{(M)}$ the left and right bounds for the numerical range $W(e^{i\theta}T)$ obtained as in (4.1). We have the following algorithm to compute the coercivity constant γ .

Algorithm 1. Computation of the coercivity constant γ .

INPUT: Bounded linear operator T , Number of approximating points N

OUTPUT: 0 or lower bound for coercivity constant γ

$W := \mathbb{C}$; $angles := \{\frac{j\pi}{N}, j = 0, \dots, N-1\}$;

foreach $\theta \in angles$ **do**

 | Compute $h_\theta^{(m)}, h_\theta^{(M)}$;

 | $W := W \cap e^{-i\theta} \{z \in \mathbb{C} : h_\theta^{(m)} \leq \operatorname{Re}\{z\} \leq h_\theta^{(M)}\}$;

end

if $0 \notin W$ **then**

 | **return** $\gamma := d(0, W)$;

else

 | $\gamma := 0$;

end

return γ ;

Algorithm 1 computes an enclosing domain $W \supset W(T)$ using N rotations of the original operator T . As $N \rightarrow \infty$ it follows from the convexity of $W(T)$ that $W \rightarrow \overline{W(T)}$. If $0 \notin W$, then the algorithm returns a positive lower bound for γ . Otherwise, either T is not coercive or N needs to be increased. If \mathcal{H} is finite dimensional, and therefore T a matrix, we can also directly compute points on the boundary of the numerical range and thereby give an interior approximation. Let $\lambda_{min}^{(\theta)}$ and $\lambda_{max}^{(\theta)}$ be the smallest, respectively largest, eigenvalue of the Hermitian part of $e^{i\theta}T$ with associated eigenvectors v_{min} and v_{max} . Then the corresponding points on the boundary of the numerical range of $W(T)$ are given by $p_{min}^{(\theta)} = \frac{\langle T v_{min}, v_{min} \rangle}{\langle v_{min}, v_{min} \rangle}$ and $p_{max}^{(\theta)} = \frac{\langle T v_{max}, v_{max} \rangle}{\langle v_{max}, v_{max} \rangle}$. It follows that the convex hull of all such points for different θ is a subset of $W(T)$, since $W(T)$ itself is convex. More information on numerical range computations can be found in [22]. An algorithm for estimating the numerical range of large and sparse matrices is described in [6].

If \mathcal{H} is infinite dimensional, then we approximate T from a finite dimensional basis $\{\chi_1, \dots, \chi_n\} \subset \mathcal{H}$ using a Galerkin approximation of T . The numerical range of T is then approximated by

$$W(T^{(h)}) = \left\{ \frac{x^H T^{(h)} x}{x^H M^{(h)} x} : x \in \mathbb{C}^n \setminus \{0\} \right\},$$

where $T^{(h)} = [\langle T\chi_j, \chi_i \rangle]$, $i, j = 1, \dots, n$, is the Galerkin projection of T and $M^{(h)} = [\langle \chi_j, \chi_i \rangle]$, the mass-matrix, is the corresponding projection of the identity in the finite dimensional basis. Hence, we need to solve generalized eigenvalue problems of the form

$$T^{(h)} x = \lambda M^{(h)} x,$$

where $T^{(h)}_H$ is the Hermitian part of $e^{i\theta} T^{(h)}$.

When solving integral equations using the Galerkin method with locally defined basis functions typically, at least in 2-d, the matrix $M^{(h)}$ has low bandwidth or is even diagonal. We, therefore, compute the Cholesky decomposition $M^{(h)} = CC^H$ to obtain the standard eigenvalue problem $C^{-1} T^{(h)}_H C^{-H} y = \lambda y$ with $y = C^H x$. This is equivalent to changing to an orthonormal basis of the Galerkin subspace.

4.2. Convergence of the numerical range of a Galerkin discretization.

In this section we analyze the convergence of the numerical range $W(T^{(h)})$ of a Galerkin discretization $T^{(h)}$ to the numerical range of $W(T)$ for a sequence of subspaces $\mathcal{V}^{(h_0)} \subset \mathcal{V}^{(h_1)} \subset \dots \subset \mathcal{H}$, where h is usually interpreted as the fineness of a boundary element discretization of an integral operator. The Galerkin discretization $T^{(h)}$ is obtained by restricting the variational problem (1.1) on \mathcal{H} to a variational problem on a finite dimensional subspace $\mathcal{V}^{(h)} \subset \mathcal{H}$. From the definition of $T^{(h)}$ as Galerkin discretization and the variational characterization of the numerical range it follows immediately that

$$W(T^{(h)}) = \{ \langle Tu, u \rangle : u \in \mathcal{V}^{(h)}, \|u\| = 1 \} \subset W(T).$$

In this section we will use the notation $d(X, Y) := \inf\{|x - y| : x \in X, y \in Y\}$ for the distance between two sets. Correspondingly, $d(x, Y) := d(\{x\}, Y)$ is the distance of a single point x to the set Y . For the analysis we need the following perturbation lemma.

LEMMA 4.1. *Let $z \in W(T)$ with associated $u \in \mathcal{H}$, $\|u\| = 1$, such that $z = \langle Tu, u \rangle$. Let $0 < \epsilon < 1$ and choose $\hat{u} \in \mathcal{H}$ with $\|u - \hat{u}\| \leq \epsilon$. Then*

$$(4.2) \quad \left| z - \frac{\langle T\hat{u}, \hat{u} \rangle}{\langle \hat{u}, \hat{u} \rangle} \right| \leq 6\|T\|\epsilon.$$

Proof. By the triangle inequality

$$(4.3) \quad \left| \langle Tu, u \rangle - \frac{\langle T\hat{u}, \hat{u} \rangle}{\langle \hat{u}, \hat{u} \rangle} \right| \leq |\langle Tu, u \rangle - \langle T\hat{u}, \hat{u} \rangle| + \left| \|\hat{u}\|^2 - \|u\|^2 \right| \frac{|\langle T\hat{u}, \hat{u} \rangle|}{\|\hat{u}\|^2}.$$

Let $f = \hat{u} - u$, i.e., $\hat{u} = u + f$. By the Cauchy-Schwarz and triangle inequalities

$$(4.4) \quad |\langle Tu, u \rangle - \langle T\hat{u}, \hat{u} \rangle| \leq \|T\| \|f\| (2 + \|f\|)$$

and

$$(4.5) \quad \left| \|\hat{u}\|^2 - \|u\|^2 \right| \leq \|f\|(2 + \|f\|).$$

Using the bounds (4.4) and (4.5) in (4.3) we find that

$$(4.6) \quad \left| z - \frac{\langle T\hat{u}, \hat{u} \rangle}{\langle \hat{u}, \hat{u} \rangle} \right| \leq 2\|T\|\|f\|(2 + \|f\|),$$

and the result (4.2) follows from the fact that $\|f\| \leq \epsilon < 1$. \square

We can now give a first convergence result. In order to state it we define the set $W_\epsilon(T) := \{z \in W(T) : d(z, \partial W(T)) \geq \epsilon\}$. Hence, for any $\epsilon > 0$ we have $W_\epsilon(T) \subset W(T)$ and $\lim_{\epsilon \rightarrow 0} d(z, W_\epsilon(T)) = 0 \forall z \in W(T)$. Also, we denote the closed convex hull of the points $z_1, \dots, z_M \in \mathbb{C}$ by $\text{conv}\{z_1, \dots, z_M\}$.

THEOREM 4.2. *Let $\mathcal{V}^{(h_\ell)}$ be an asymptotically dense sequence of finite dimensional subspaces of \mathcal{H} such that $\mathcal{V}^{(h_0)} \subset \mathcal{V}^{(h_1)} \subset \dots \subset \mathcal{H}$. Denote by $T^{(h_\ell)}$ the associated Galerkin discretization of T . For any $\epsilon > 0$ there exists $m \in \mathbb{N}$ such that $W_\epsilon(T) \subset W(T^{(h_j)}) \subset W(T)$ for any $j \geq m$.*

Proof. Without restriction let $0 < \epsilon \leq 1$. The case of larger ϵ follows from this since $W_{\epsilon_1}(T) \subset W_{\epsilon_2}(T)$ for $\epsilon_1 \geq \epsilon_2$. Choose a finite number of M points z_j in $W(T) \setminus W_\epsilon(T)$ such that for $Z = \text{conv}\{z_1, \dots, z_M\}$ we have $W_\epsilon(T) \subset Z$ and $d(\partial W_\epsilon(T), \partial Z) > 0$. This is possible due to the convexity of $W(T)$. Now choose $0 < \delta < 6\|T\|$ small enough, such that for any set $Z_\delta = \text{conv}\{\hat{z}_1, \dots, \hat{z}_M\}$ with \hat{z}_j satisfying $|z_j - \hat{z}_j| \leq \delta$ it holds that $W_\epsilon(T) \subset Z_\delta$. Hence, perturbing the points z_j by at most δ still results in a convex set that encloses $W_\epsilon(T)$. Denote by $u_j \in \mathcal{H}$, $\|u_j\| = 1$, elements of \mathcal{H} associated with z_j such that $z_j = \langle Tu_j, u_j \rangle$ and choose $m \in \mathbb{N}$ sufficiently large such that there exists $\hat{u}_j \in \mathcal{V}^{(h_m)} \setminus \{0\}$ with $\|u_j - \hat{u}_j\| \leq \delta/(6\|T\|)$ for all $1 \leq j \leq M$. The existence of such an m follows from the asymptotic density of the subspaces $\mathcal{V}^{(h_\ell)}$ in \mathcal{H} . From Lemma 4.1 and the choice of δ , it follows now that for the points $\hat{z}_j = \frac{\langle T\hat{u}_j, \hat{u}_j \rangle}{\langle \hat{u}_j, \hat{u}_j \rangle}$ we have $W_\epsilon(T) \subset \text{conv}\{\hat{z}_1, \dots, \hat{z}_M\}$. Furthermore, from $\hat{z}_j \in W(T^{(h_m)})$ and the convexity of the numerical range we have $W_\epsilon(T) \subset W(T^{(h_m)})$ and, due to the definition of the subspaces $\mathcal{V}^{(h_j)}$, also $W_\epsilon(T) \subset W(T^{(h_\ell)}) \subset W(T)$ for any $\ell \geq m$. \square

Remark 4.3. It follows from Theorem 4.2 that every point in the interior of $W(T)$ also belongs to the numerical range of a sufficiently fine Galerkin discretization. Hence, the main difference between the numerical range of a Galerkin discretization and that of the original operator T is the behavior of their boundaries. Indeed, $T^{(h)}$ is finite dimensional, and hence $W(T^{(h)})$ is closed. However, $W(T)$ is, in general, neither open nor closed.

We now prove a simple convergence estimate for the numerical range of a boundary integral operator based on a Galerkin boundary element discretization with piecewise constant elements of diameter h . To express the convergence result let $\Delta_\nu := \{z \in \mathbb{C} : |z| \leq \nu\}$. Also, for two sets $A, B \subset \mathbb{C}$ let $A + B := \{a + b : a \in A, b \in B\}$.

THEOREM 4.4. *Let Ω be a piecewise smooth Lipschitz domain with boundary Γ , and let $T : L^2(\Gamma) \rightarrow L^2(\Gamma)$ be a bounded linear operator. Denote by $T^{(h)}$ its Galerkin discretization from a space $\mathcal{V}^{(h)}$ of piecewise constant elements of diameter at most h . Then $W(T^{(h)}) \subset W(T)$ and for any $\epsilon > 0$ and $0 < \alpha \leq 1$ there exists $C > 0$, which depends on T , ϵ , and α such that*

$$W_\epsilon(T) \subset W(T^{(h)}) + \Delta_{Ch^\alpha}$$

for any h sufficiently small.

Proof. As in the proof of Theorem 4.2 we choose M points in $W(T) \setminus W_\epsilon(T)$ such that $W_\epsilon(T) \subset Z := \text{conv}\{z_1, \dots, z_M\}$ and $d(\partial W_\epsilon(T), \partial Z) > 0$. Denote by $u_j \in L^2(\Gamma)$, $\|u_j\|_{L^2(\Gamma)} = 1$, functions associated with z_j , such that $z_j = \langle Tu_j, u_j \rangle$. Also, as in the proof of Theorem 4.2, let $0 < \delta < 6\|T\|_{L^2(\Gamma)}$ be small enough such that for every $Z_\delta := \text{conv}\{\hat{z}_1, \dots, \hat{z}_M\}$ with $|z_j - \hat{z}_j| \leq \delta$ we have $W_\epsilon(T) \subset Z_\delta$.

Since Γ is a Lipschitz boundary, the Sobolev space $H^\alpha(\Gamma)$ is well defined for $0 < \alpha \leq 1$. Also, $H^\alpha(\Gamma)$ is dense in $L^2(\Gamma)$. Hence, there exist functions $\hat{u}_j \in H^\alpha(\Gamma) \setminus \{0\}$, such that $\|u_j - \hat{u}_j\|_{L^2(\Gamma)} \leq \delta/(6\|T\|_{L^2(\Gamma)})$. From Lemma 4.1 it now follows that $|z_j - \hat{z}_j| \leq \delta$ for $\hat{z}_j = \frac{\langle T\hat{u}_j, \hat{u}_j \rangle}{\langle \hat{u}_j, \hat{u}_j \rangle}$, and therefore, $W_\epsilon(T) \subset \text{conv}\{\hat{z}_1, \dots, \hat{z}_M\}$.

Note that rescaling the functions \hat{u}_j does not change the values \hat{z}_j and the relationship $|z - \hat{z}_j| \leq \delta$. Without restriction we can, therefore, rescale the functions \hat{u}_j to $\|\hat{u}_j\|_{L^2(\Gamma)} = 1$. By approximation results for piecewise constant basis functions [38, Theorem 10.2] there exists $\hat{u}_j^{(h)} \in \mathcal{V}^{(h)}$ such that

$$(4.7) \quad \|\hat{u}_j - \hat{u}_j^{(h)}\|_{L^2(\Gamma)} \leq Ch^\alpha |\hat{u}_j|_{H^\alpha(\Gamma)},$$

$j = 1, \dots, M$, for some $C > 0$ independent of j and h . Let $L := \max_j |\hat{u}_j|_{H^\alpha(\Gamma)}$. For the points $\hat{z}_j^{(h)} = \frac{\langle T\hat{u}_j^{(h)}, \hat{u}_j^{(h)} \rangle}{\langle \hat{u}_j^{(h)}, \hat{u}_j^{(h)} \rangle}$ it follows from Lemma 4.1 that $|\hat{z}_j - \hat{z}_j^{(h)}| \leq 6\|T\|Ch^\alpha L$ if h is sufficiently small, such that $Ch^\alpha L < 1$. Subsuming the constants in C we have

$$(4.8) \quad |\hat{z}_j - \hat{z}_j^{(h)}| \leq Ch^\alpha$$

for some $C > 0$. It follows that the boundary of the convex hull of the points \hat{z}_j and the boundary of the convex hull of the points $\hat{z}_j^{(h)}$ also have a distance bounded by Ch^α for some $C > 0$, and therefore, by the choice of the points \hat{z}_j ,

$$W_\epsilon(T) \subset \text{conv}\{\hat{z}_1, \dots, \hat{z}_M\} \subset \text{conv}\{\hat{z}_1^{(h)}, \dots, \hat{z}_M^{(h)}\} + \Delta_{Ch^\alpha}.$$

From the convexity of the numerical range we have $\text{conv}\{\hat{z}_1^{(h)}, \dots, \hat{z}_M^{(h)}\} \subset W(T^{(h)})$ giving

$$W_\epsilon(T) \subset W(T^{(h)}) + \Delta_{Ch^\alpha}.$$

The statement $W(T^{(h)}) \subset W(T)$ follows trivially from the variational characterization of the numerical range. \square

Remark 4.5. Asymptotically, the rate of convergence in Theorem 4.4 is $O(h)$. But in practice the constant C may be large if the \hat{u}_j are measured in the $H^1(\Gamma)$ norm. If \hat{u}_j is better represented in $H^\alpha(\Gamma)$ for some $\alpha < 1$, then numerically we may only see convergence of the rate $O(h^\alpha)$. However, for sufficiently small h the rate of convergence will eventually approach $O(h)$. An example is given in section 5.1.

A slight improvement on the convergence rate of Theorem 4.4 can be obtained using properties of the Galerkin approximations. However, we will see that this only applies to the boundary integral operator A on domains which are smoother than just Lipschitz: we prove that $C^{2,\beta}$, $0 < \beta \leq 1$, is sufficient. In addition the operator must be self-adjoint; however, this is not restrictive since, as shown earlier, we can compute $W(T)$ by considering only the Hermitian part T_H . We first prove a refinement of Lemma 4.1 in the case where \hat{u} is the best approximation of u .

LEMMA 4.6. *Let X be a bounded linear operator on \mathcal{H} that is self-adjoint: $X^* = X$. Let $z \in W(X)$ with associated $u \in \mathcal{H}$, $\|u\| = 1$, such that $z = \langle Xu, u \rangle$. Let $\mathcal{V}^{(h)}$ be a finite dimensional subspace of \mathcal{H} , and let $u^{(h)}$ denote the best approximation to u from $\mathcal{V}^{(h)}$ defined by*

$$(4.9) \quad \langle u^{(h)} - u, v^{(h)} \rangle = 0 \quad \forall v^{(h)} \in \mathcal{V}^{(h)}.$$

Then

$$(4.10) \quad \left| z - \frac{\langle Xu^{(h)}, u^{(h)} \rangle}{\langle u^{(h)}, u^{(h)} \rangle} \right| \leq \|u - u^{(h)}\| \left(\|Xu - (Xu)^{(h)}\| + \|Xu^{(h)} - (Xu^{(h)})^{(h)}\| + \|X\| \|u - u^{(h)}\| \right),$$

where $(Xu^{(h)})^{(h)}$ and $(Xu)^{(h)}$ are the best approximations of $Xu^{(h)}$ and Xu , respectively, from $\mathcal{V}^{(h)}$.

Proof. From the proof of Lemma 4.1 we have that (4.3) holds with T replaced by X . Instead of using the bounds (4.4) and (4.5) (with T replaced by X) in (4.3), we use the equations

$$(4.11) \quad \langle Xu, u \rangle - \langle Xu^{(h)}, u^{(h)} \rangle = \langle Xu - (Xu)^{(h)}, u - u^{(h)} \rangle + \langle u - u^{(h)}, Xu^{(h)} - (Xu^{(h)})^{(h)} \rangle$$

and

$$(4.12) \quad \langle u^{(h)}, u^{(h)} \rangle - \langle u, u \rangle = \langle u - u^{(h)}, u - u^{(h)} \rangle,$$

and then using the Cauchy–Schwarz inequality yields the result (4.10).

Equations (4.11) and (4.12) are consequences of the best approximation property (4.9) and the fact that X is self-adjoint. Indeed

$$\begin{aligned} \langle Xu, u \rangle - \langle Xu^{(h)}, u^{(h)} \rangle &= \langle Xu, u - u^{(h)} \rangle - \langle X(u^{(h)} - u), u^{(h)} \rangle \\ &= \langle Xu, u - u^{(h)} \rangle - \langle u^{(h)} - u, Xu^{(h)} \rangle \end{aligned}$$

by $X = X^*$, and using the property (4.9) to subtract off $(Xu)^{(h)}$ and $(Xu^{(h)})^{(h)}$ from the first and second brackets, respectively, yields (4.11). Property (4.9) also implies

$$\langle u^{(h)}, u^{(h)} \rangle = \langle u, u^{(h)} \rangle = \langle u^{(h)}, u \rangle,$$

which gives (4.12). \square

The key point about (4.10) is that each term on the right-hand side is the product of two best approximation errors; thus the Galerkin approximation to the functional $\langle u, Xu \rangle$ converges faster than $\|u - u^{(h)}\|$ —this is an example of superconvergence. Another example of Galerkin approximations of functionals exhibiting superconvergence is given in [36]. Using Lemma 4.5 instead of Lemma 4.1 we can now prove a refined version of Theorem 4.4 for the numerical range of self-adjoint operators.

THEOREM 4.7. *Let Ω be a Lipschitz domain with boundary Γ , and let $X : L^2(\Gamma) \rightarrow L^2(\Gamma)$ be a self-adjoint bounded linear operator that also maps $H^1(\Gamma)$ to $H^1(\Gamma)$. Denote by $X^{(h)}$ its Galerkin discretization from a space $\mathcal{V}^{(h)} \subset L^2(\Gamma)$ of piecewise constant elements of diameter at most h . Then $W(X^{(h)}) \subset W(X)$ and for any $\epsilon > 0$ there exists $C > 0$ (depending on X and ϵ), such that*

$$W_\epsilon(X) \subset W(X^{(h)}) + \Delta_{Ch^2}$$

for any h sufficiently small.

Proof. This is identical to that of Theorem 4.4 for the case $\alpha = 1$ except that now Lemma 4.6 gives that

$$|\hat{z}_j - \hat{z}_j^{(h)}| \leq Ch^2$$

for some $C > 0$. The requirement that $X : H^1(\Gamma) \rightarrow H^1(\Gamma)$ is necessary to apply the interpolation result (4.7) to $X\hat{u}_j$ and $X\hat{u}_j^{(h)}$. \square

We now prove that the approximation of the numerical range of $A_{k,\eta}$ also shows superconvergence if Γ is sufficiently smooth. We need the following two lemmas.

LEMMA 4.8. *If Γ is $C^{2,\beta}$, $0 < \beta \leq 1$, then the operators $A_H := \frac{1}{2}(A_{k,\eta} + A_{k,\eta}^*)$ and $A_S := \frac{1}{2i}(A_{k,\eta} - A_{k,\eta}^*)$, where $A_{k,\eta}$ is given by (1.9) and $A_{k,\eta}^* = \overline{A'_{k,\eta}}$, where $A'_{k,\eta}$ is given by (2.1), map $L^2(\Gamma) \rightarrow L^2(\Gamma)$ and $H^1(\Gamma) \rightarrow H^1(\Gamma)$*

Proof. Certainly if S_k, K_k , and K'_k all map $L^2(\Gamma) \rightarrow L^2(\Gamma)$ and $H^1(\Gamma) \rightarrow H^1(\Gamma)$, then so do A_H and A_S . When Γ is Lipschitz

$$\begin{aligned} S_k &: H^{s-1/2}(\Gamma) \rightarrow H^{s+1/2}(\Gamma), \\ K'_k &: H^{s-1/2}(\Gamma) \rightarrow H^{s-1/2}(\Gamma), \\ K_k &: H^{s+1/2}(\Gamma) \rightarrow H^{s+1/2}(\Gamma) \end{aligned}$$

for $|s| \leq 1/2$ [30, Theorem 7.1]. Thus all three map $L^2(\Gamma) \rightarrow L^2(\Gamma)$, but only S_k and K_k map $H^1(\Gamma) \rightarrow H^1(\Gamma)$. By [16, Theorem 3.6], if Γ is $C^{2,\beta}$, $0 < \beta \leq 1$, then $K'_k : L^2(\Gamma) \rightarrow H^1(\Gamma)$ and thus maps $H^1(\Gamma) \rightarrow H^1(\Gamma)$. \square

LEMMA 4.9. *Let Γ be $C^{2,\beta}$, $0 < \beta \leq 1$. Let $A_{k,\eta}^{(h)}$ be the Galerkin discretization of $A_{k,\eta}$ from a space $\mathcal{V}^{(h)} \subset L^2(\Gamma)$ of piecewise constant elements of diameter at most h and denote by $u^{(h)} \subset \mathcal{V}^{(h)}$ the Galerkin approximation of $u \in L^2(\Gamma)$. Denote by z and $z^{(h)}$ the corresponding points in the numerical range of $A_{k,\eta}$, respectively $A_{k,\eta}^{(h)}$, given by*

$$z := \frac{\langle A_{k,\eta}u, u \rangle}{\langle u, u \rangle}, \quad z^{(h)} := \frac{\langle A_{k,\eta}u^{(h)}, u^{(h)} \rangle}{\langle u^{(h)}, u^{(h)} \rangle}.$$

Then we have

$$(4.13) \quad |z - z^{(h)}| \leq Ch^2$$

for some $C > 0$ independent of u and h .

Proof. Splitting up $A_{k,\eta}$ into A_H and A_S as defined in Lemma 4.8 gives

$$z = \frac{\langle A_H u, u \rangle}{\langle u, u \rangle} + i \frac{\langle A_S u, u \rangle}{\langle u, u \rangle}.$$

From Lemma 4.8 it follows that Lemma 4.6 can be applied separately to the real and imaginary parts of z and $z^{(h)}$ resulting in (4.13). \square

By using the approximation result (4.13) in the proof of Theorem 4.4 we immediately obtain the following $O(h^2)$ convergence result for the numerical range of the operator $A_{k,\eta}$.

THEOREM 4.10. *Let the assumptions of Lemma 4.9 hold. Then for any $\epsilon > 0$ there exists $C > 0$ (depending on $A_{k,\eta}$ and ϵ) such that $W(A_{k,\eta}^{(h)}) \subset W(A_{k,\eta})$ and*

$$W_\epsilon(A_{k,\eta}) \subset W(A_{k,\eta}^{(h)}) + \Delta_{Ch^2}$$

for any h sufficiently small.

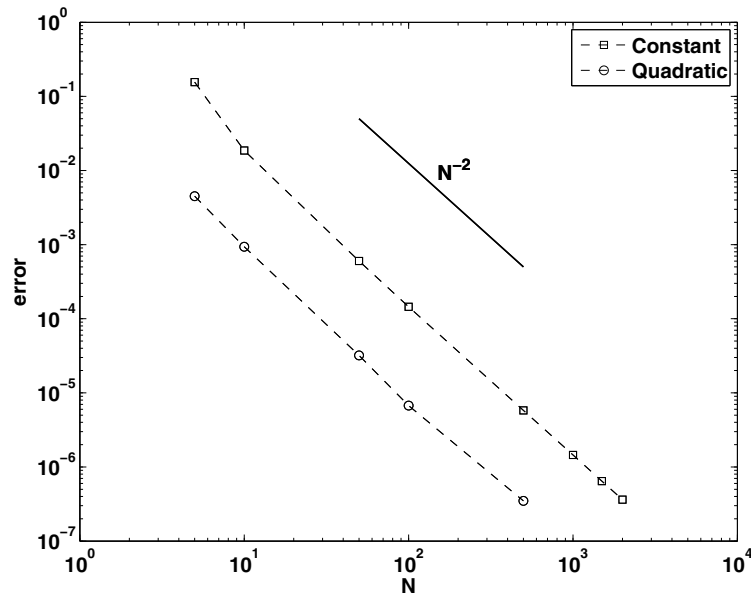


FIG. 5.1. Convergence of the coercivity constant for a growing number of elements per wavelength on the unit circle for $k = 1$ with constant and quadratic basis functions.

5. Numerical examples. In this section we demonstrate the convergence of the numerical range and the coercivity constant as $h \rightarrow 0$ and apply the numerical range computation to test the coercivity of the integral operator A for several interesting domains. For simplicity, we take the most commonly used choice of coupling constant, $\eta = k$ and omit the indices in $A_{k,\eta}$ since the k -dependence is clear from the context.

5.1. Convergence of the numerical range as $h \rightarrow 0$. We start by demonstrating the convergence results of section 4.2. Consider the operator A on the unit circle with $k = 1$. For the boundary element discretization we decompose the unit circle into elements of equal length h and choose piecewise constant basis functions on each element. We approximate the numerical range of $A^{(h)}$ with the exterior approximation algorithm described in section 4.1 using 50 eigenvalue computations, resulting in an approximating polygon with 100 corners. An approximation for the coercivity constant $\gamma^{(h)}$ of $A^{(h)}$ is then given as the distance of the exterior polygon to the origin. The rate of convergence for decreasing h is shown in Figure 5.1. For smooth domains, such as the circle, with boundary length L we use approximately $\frac{NLk}{2\pi}$ elements; that is, $h \approx \frac{2\pi}{Nk}$. For polygonal domains considered later, L is the length of a boundary segment. Hence, h can differ on each segment. With this notation $N = 10$ corresponds to the rule of thumb of 10 elements per wavelength. The error for the coercivity constant of the circle is measured as $|\gamma^{(h)} - 1|$ since it is known that for sufficiently large k the exact coercivity constant is 1. Indeed, the convergence curve seems to confirm this result for the wavenumber $k = 1$. With piecewise constant basis functions the convergence is approximately quadratic as suggested by Theorem 4.7. For comparison we also give the rate of convergence using piecewise quadratic basis functions. In this case, even with just 10 elements per wavelength the approximate coercivity constant has an error of less than 1%. The observed rate of convergence stays quadratic. Standard results for approximation in Sobolev spaces with higher

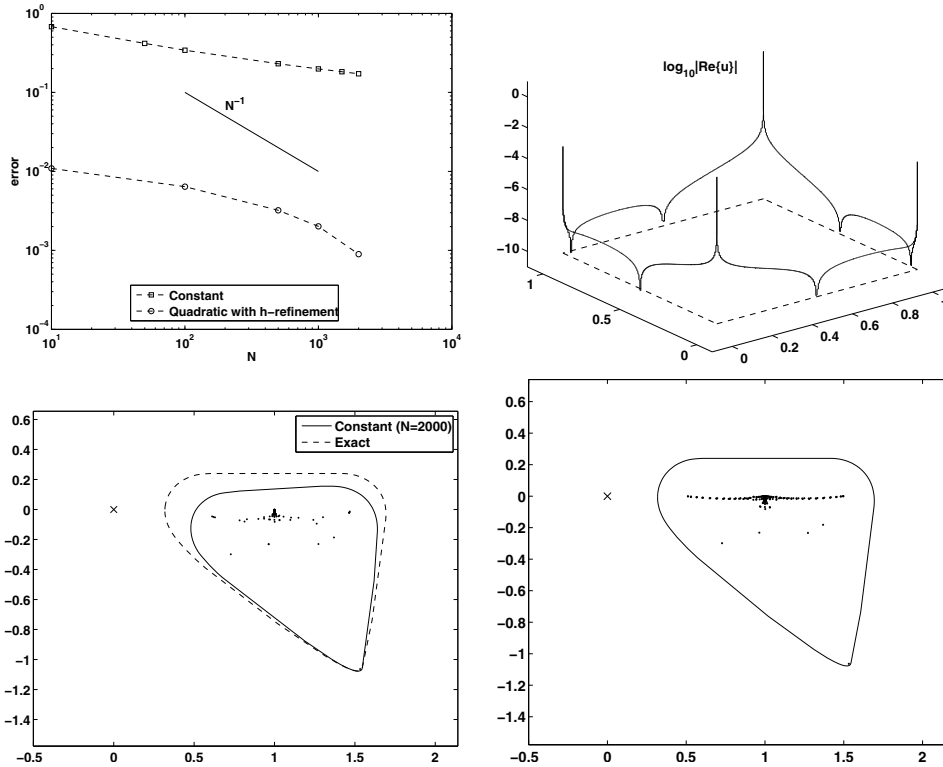


FIG. 5.2. Upper left: Rate of convergence of $\gamma^{(h)}$ on the unit square. Upper right: A function associated with a point of the numerical range close to 0.5. Lower left: Approximate numerical range using piecewise constant basis functions (solid line) against exact numerical range (dotted line). The dots show the eigenvalues of the Galerkin projection $A^{(h)}$. Lower right: Approximation to exact numerical range and the spectrum of A on the square obtained by using piecewise quadratic basis functions and h -refinement towards corners of the square.

order basis functions [21, Theorem 3.1] would suggest asymptotically a faster rate of convergence. However, a full analysis of the observed convergence involves a careful estimation of the constants involved in the error bounds as $\epsilon \rightarrow 0$ in the theorems of section 4.2 and is beyond the scope of this paper.

We now consider the approximation of the coercivity constant of A on the unit square. Again, we choose $k = 1$. The convergence of the coercivity constant for approximations with piecewise constant basis functions is shown in the upper left plot of Figure 5.2 (square-dotted line). The observed convergence is much slower than the expected maximum asymptotic rate of $O(h)$ from Theorem 4.4. The reason is shown in the upper right plot of Figure 5.2. It shows the logarithmic plot of a function on the boundary Γ that is associated with a point in the numerical range close to 0.5. It was computed as an eigenfunction of a Galerkin discretization of A with piecewise quadratic basis functions and exponential h -refinement towards the corners. It has a large $H^1(\Gamma)$ norm, indicating that the constants of the estimate in Theorem 4.4 will become large for $\alpha = 1$. Hence, this function is much better represented as a function in $H^\alpha(\Gamma)$ for some $\alpha < 1$ and we expect the visible numerical rate of convergence to be $O(h^\alpha)$, even though eventually the asymptotic rate will approach $O(h)$. The lower left plot of Figure 5.2 shows the effect on the shape of the numerical range. With

$N = 2000$ (that is, roughly 2000 elements per wavelength), the numerical range of the discretization only fills parts of the exact numerical range, leading to an overestimation of the coercivity constant. The (up to plotting accuracy) correct numerical range was obtained by using piecewise quadratic basis functions together with exponential h -refinement towards corners. The lower right plot shows the approximate spectrum (black dots) and the boundary of the numerical range obtained with this strategy. The convergence of the coercivity constant $\gamma^{(h)}$ for the refined discretizations is shown as the circle-dotted line in the upper left plot of Figure 5.2. N means here that approximately N elements per wavelength were used until a distance of $\frac{2\pi}{Nk}$ away from the corner together with exponential h -refinement in the direct neighborhood around the corner. This gives an accuracy of around 10^{-2} for $N = 10$. The best obtained value for the coercivity constant on the square is 0.318 using $N = 3000$. As comparison for $N = 10$ we obtain 0.329, a relative distance of less than 4% to the best value. On the plotting scale there is no significant difference between the numerical range for $N = 10$ and for $N = 3000$ using the exponential refinement close to the corners.

5.2. Numerical range and coercivity constant for growing k . In this section we numerically investigate the behavior of the numerical range and the coercivity constant for growing wavenumber k of the integral operator A for the boundaries of several polygonal and smooth domains.

For smooth domains we used boundary element discretizations with piecewise quadratic basis functions, and for cornered domains we additionally applied exponential h -refinement towards the corners. Typically we used between 10 and 20 elements per wavelength away from the corners depending on the overall system size. Whenever possible within the limit of the available memory and feasible computing times we checked the accuracy by refining h . At least on the level of plotting accuracy we always found good agreement between the results for 10 elements per wavelength and higher values for the number of elements. All computations were done using a self-developed C++ code, which is OpenMP parallelized. It ran on an 8 core Linux workstation with 64GB RAM. The finest discretizations that were still feasible in terms of computing time led to matrix problems of dimensions between ten and eleven thousand. Since 50 eigenvalue decompositions of the Hermitian part of complex rotations of the operator needed to be performed to obtain an approximating polygon for the numerical range with 100 corners, the overall computing time was roughly in the range of 12 to 20 hours for the largest matrix problems. Due to the cubic dependence of the computing time for the full matrix problems on the dimension of the matrices, doubling the number of elements leads to an additional factor 8 in time.

5.2.1. Smooth domains. For the unit circle coercivity was already shown for sufficiently large k in [17]. Therefore, for this domain we are more interested in what happens as $k \rightarrow 0$. In Figure 5.3, we show the numerical ranges on the unit disk for $k = 10, 1, 0.1, 0.01$. The corresponding values of the coercivity constant γ are given in the following table:

k	0.01	0.1	1	10
γ	0.10	0.57	1.00	1.00

For $k = 1$ and above the coercivity constant indeed seems to be 1. However, as $k \rightarrow 0$ the numerical range starts deteriorating into a line and it appears that also $\gamma \rightarrow 0$. This is consistent with the fact that the choice $\eta = k$ is not optimal for

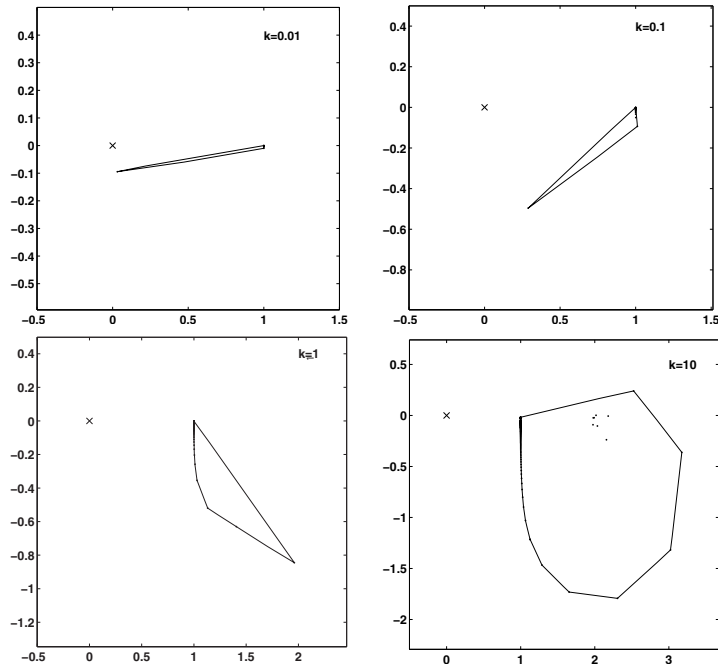


FIG. 5.3. The numerical range of A on the unit circle for $k = 0.01, 0.1, 1, 10$. The black dots are approximations to the spectral values of A .

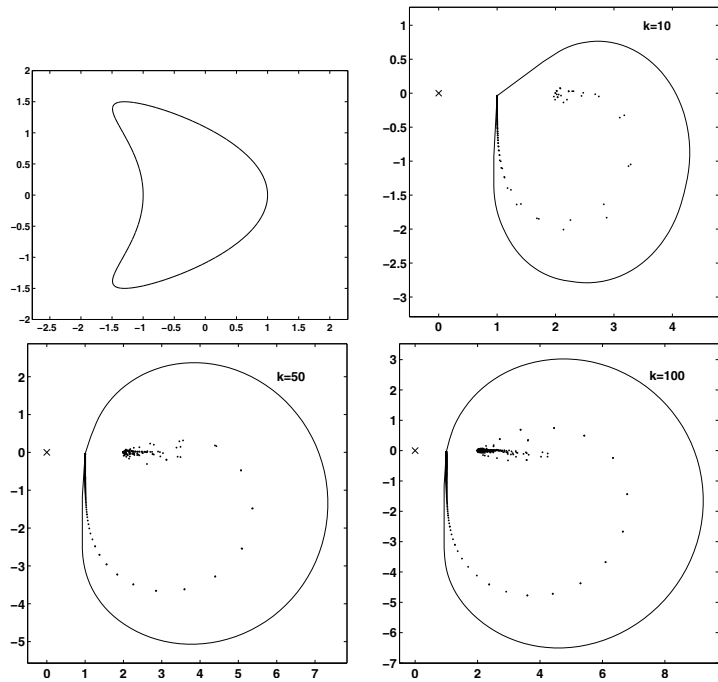


FIG. 5.4. The numerical range of A on a kite shape (upper left plot) for $k = 10, 50, 100$.

small wavenumbers (see section 2), and also with the fact that $A_0 = I + K'_0$ is not invertible, and hence not coercive, on $L^2(\Gamma)$ for any Lipschitz domain since it maps any L^2 function into one with zero mean and hence is not surjective [43]. However, if we fix $\eta = 1$, then for $k = 0.1$ and $k = 0.01$ we obtain that the coercivity constant is 1. Since the eigenvalues of A on the unit circle are explicitly known (see, for example, [17]), and the numerical range is just the convex hull of the spectrum in this case, one may also approximate the coercivity constant for the unit circle directly without using a Galerkin discretization of the operator. Also, it is interesting to note that for growing k more and more eigenvalues cluster around the point 2 (see Figure 3.1). However, for each k there can be only a finite number of eigenvalues close to 2 since A on the unit circle is a compact perturbation of the identity; therefore, the only accumulation point of the eigenvalues is 1.

The next domain is a kite shape. A parametrization of its boundary is given by $Z(t) = \cos t + 0.65 \cos 2t - 0.65 + 1.5i \sin t$, $t \in [0, 2\pi]$. The numerical range for $k = 10, 50, 100$ is shown in Figure 5.4. Again, as in the case of the unit circle, there are more and more eigenvalues appearing close to 2 as k becomes larger. However, the main difference between this domain and the circle is that the operator A is not normal since the numerical range is not just the convex hull of the eigenvalues. But interestingly we still have $\gamma \approx 1$ for all three cases. Again, the coercivity constant seems to be independent of the wavenumber for sufficiently large k . The size of the numerical range grows as k becomes larger. This is due to the norm bound (2.5) and the equivalence of the numerical radius and the norm of A in (3.2).

In the next example we show results for a domain that, like the kite, is nonconvex and star-shaped, but for which the coercivity constant of A behaves very differently as k grows. It is an inverted ellipse defined by $Z(t) = \frac{e^{it}}{1 + \frac{1}{2}e^{2it}}$, $t \in [0, 2\pi]$. Both the inverted ellipse and the corresponding numerical range of A for $k = 10, 50, 100$ are shown in Figure 5.5. The following table shows approximations of the coercivity constant γ for the different wavenumbers:

k	10	50	100	200
γ	0.988	0.737	0.672	0.585

It is striking that, in contrast to the circle and the kite shape, γ is not independent of k in this range. It is an open question whether there is a lower bound $C > 0$, such that $\gamma > C$ for all k on the inverted ellipse or whether $\gamma \rightarrow 0$ as $k \rightarrow \infty$ (see also the discussion in section 6).

5.2.2. Polygonal domains. We start with two simple convex polygons, namely the unit square and the equilateral triangle. For the unit square and $k = 1$ a plot of the numerical range was already shown in Figure 5.2. We now present results for growing k . Figure 5.6 shows the numerical range and approximations of the spectra for A on the square in the case of the wavenumbers $k = 10, 50, 100$. The lower right plot shows a comparison of the numerical range in all three cases. Again, due to (2.6) and (3.2) the size of the numerical range grows for growing k . For γ we obtain in all three cases the approximation $\gamma \approx 0.328$. It is interesting to note that close to the origin for all three wavenumbers the boundary of the numerical range is almost identical (see the lower right plot of Figure 5.6). For $k = 1$ we computed a value of $\gamma \approx 0.318$ using approximately 3000 elements per wavelength while here we used around 20 elements per wavelength. Hence, the value of γ for the higher wavenumbers has a relative distance of around 3% to the value for $k = 1$, which is likely due to the

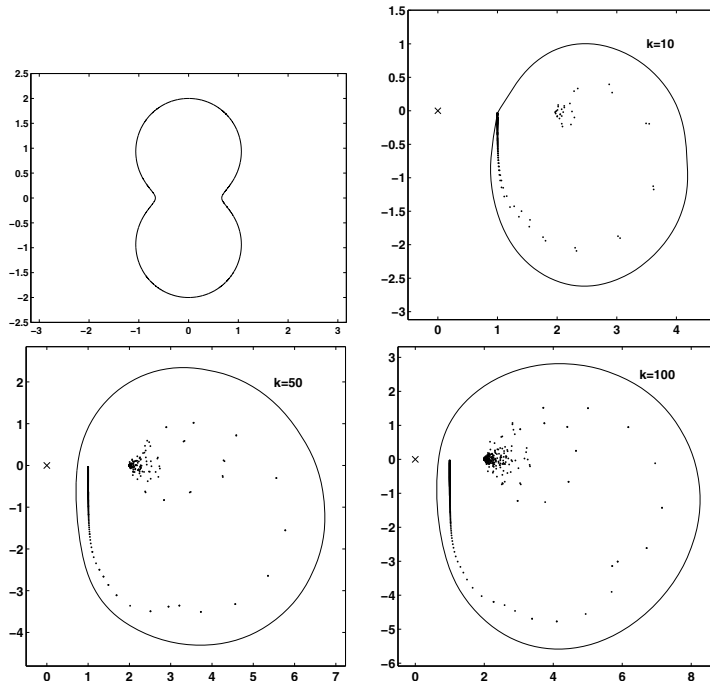


FIG. 5.5. An inverted ellipse and the associate numerical range of A for $k = 10, 50, 100$.

higher discretization error (note that for 10 elements per wavelength we reported a value of 0.329 in section 5.1).

As Figure 5.7 shows, the operator A on the equilateral triangle behaves very similarly to the square. Again, the computed coercivity constant does not seem to change as the wavenumber varies. For the three considered wavenumbers $k = 10, 50, 100$ we have $\gamma \approx 0.17$.

The square and the triangle are both convex domains, and both exhibit numerical wavenumber independence of γ . To see that this feature is not restricted to convex polygonal domains consider the L-shape in Figure 5.8. Again, the coercivity constant seems to be independent of the wavenumber with a value of $\gamma \approx 0.30$. Figure 5.9 shows the results for a polygon (the “double-L”) that is not only nonconvex, but is also nonstar-shaped, and again the results are very similar to the other domains. In this example we have $\gamma \approx 0.30$ for all three wavenumbers, which interestingly is, up to numerical accuracy, identical to the value for the L-shape.

5.3. A trapping domain. Our last example is the trapping domain shown in Figure 5.10, so-called because the open cavity can “trap” high frequency waves. That is, we expect there to be asymptotically trapped modes of the PDE (1.5) in the cavity for large wavenumbers k that are multiples of 5 (since the width of the cavity is $\pi/5$). This fact was used in [12] to show that for this domain $\|A^{-1}\|$ satisfies (2.4) when k_n is a multiple of 5, and hence the operator A cannot be uniformly coercive for large k . Figure 5.11 shows the numerical range of A for this domain in the cases $k = 4, 5, 8, 10$. For $k = 4$ and $k = 8$ the operator A is coercive, but for $k = 5$ and $k = 10$ we lose coercivity. Moreover, for *all* wavenumbers in Figure 5.11 the spectrum of A is in the right half-plane independent of whether the operator is coercive or not. This again

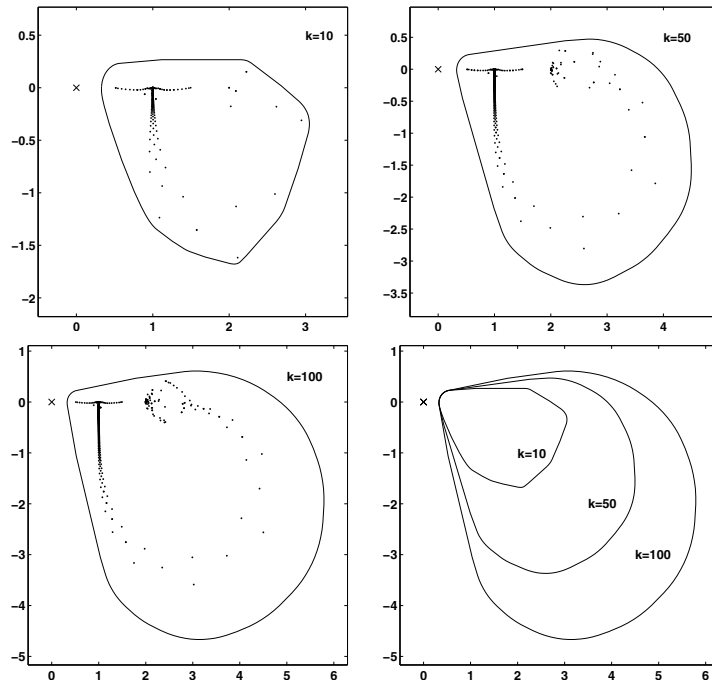


FIG. 5.6. The numerical range of A on the unit square for $k = 10, 50, 100$. The black dots are approximations to the spectral values of A . The lower right plot shows a comparison of the numerical ranges for the three different wavenumbers.

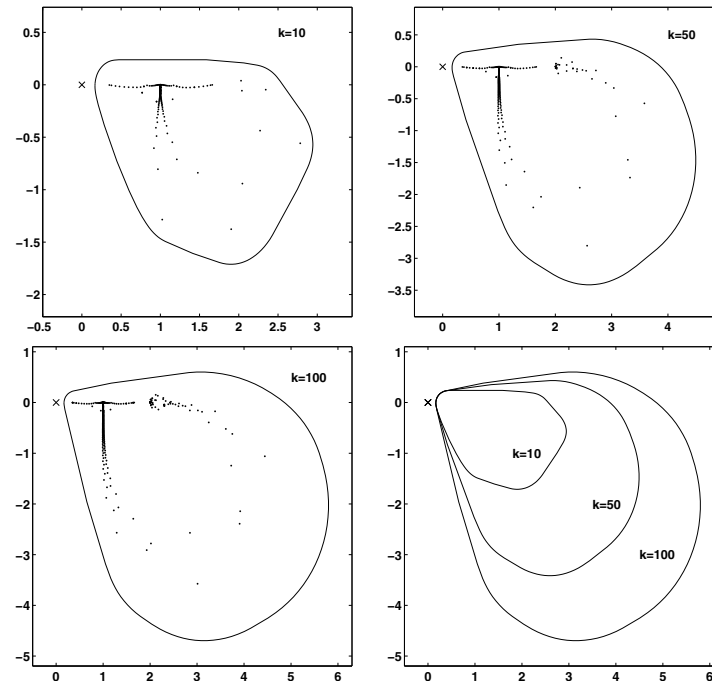


FIG. 5.7. The numerical range of A on the equilateral triangle with sides of unit length for $k = 10, 50, 100$.

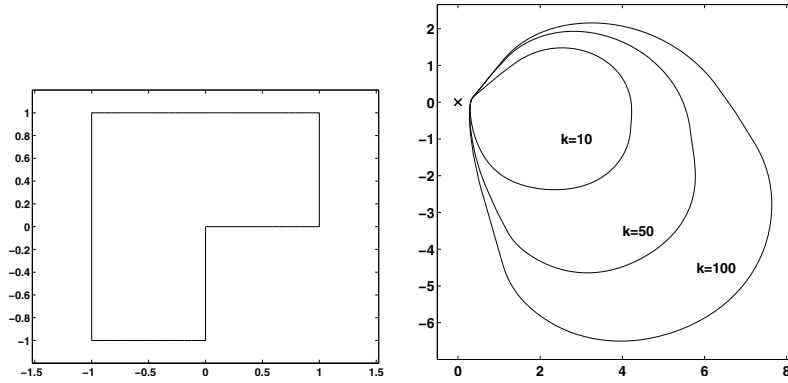


FIG. 5.8. The numerical range for $k = 10, 50, 100$ of A for the L -shaped domain.

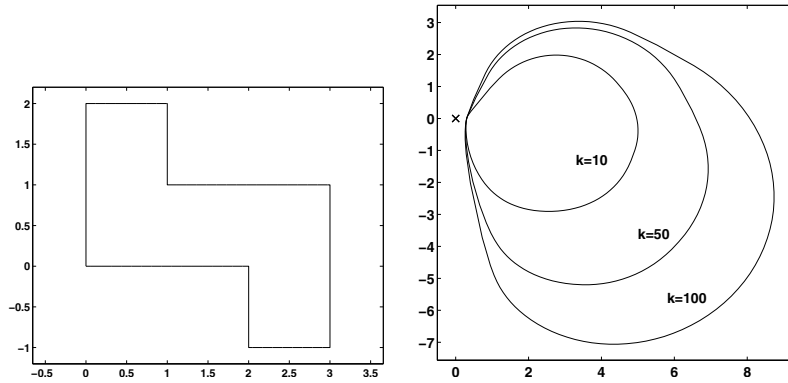


FIG. 5.9. The numerical range for $k = 10, 50, 100$ of A for a nonstar-shaped domain (“double- L ”).

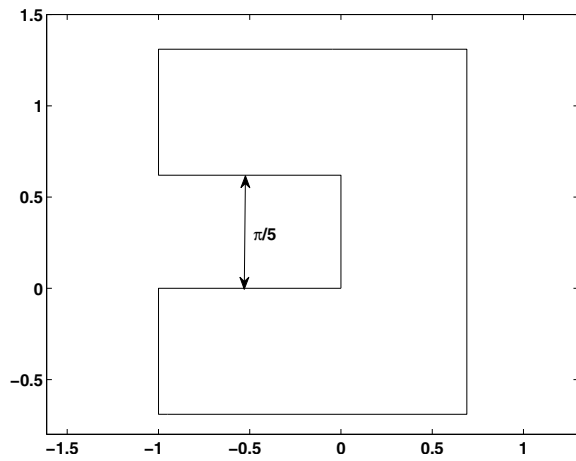


FIG. 5.10. A trapping domain. The open cavity has a width of $\pi/5$.

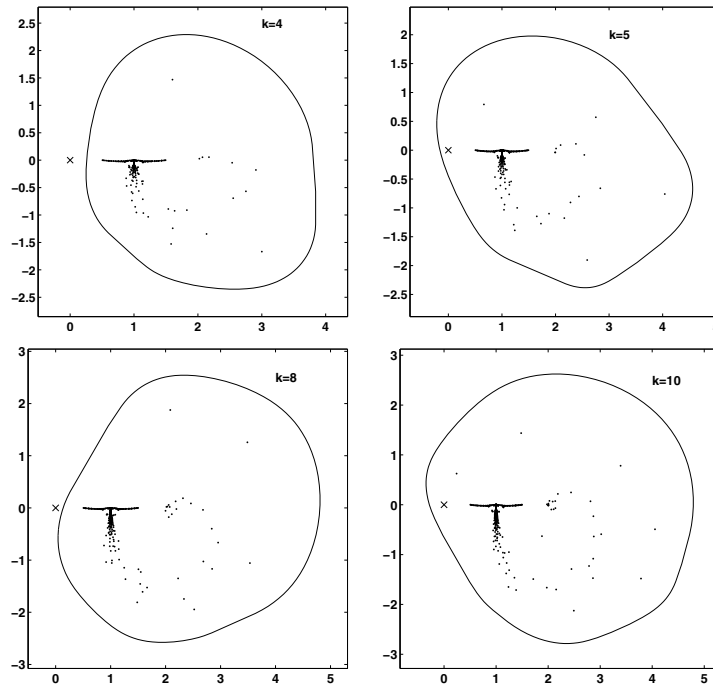


FIG. 5.11. The numerical range of A for the trapping domain from Figure 5.10 in the cases $k = 4, 5, 8, 10$.

suggests that spectral information is not sufficient to understand coercivity. We now give a possible explanation for the loss of coercivity at $k = 5$ and $k = 10$ by considering resonances of the exterior scattering problem.

We now allow the wavenumber k to be complex instead of just real, and for simplicity we take $\operatorname{Re}\{k\} > 0$. For any η and $k \in \mathbb{C}$, $A_{k,\eta} : L^2(\Gamma) \rightarrow L^2(\Gamma)$ and is Fredholm with index zero [13, Theorem 2.7]. What follows below is valid for values of η satisfying (i) $\operatorname{Re}\{\eta k\} > 0$, and (ii) η is an analytic function of k . The first condition is to ensure that $A_{k,\eta}$ is bijective for $\operatorname{Im}\{k\} > 0$ (the proof is a simple extension of the proof for real k in [13, Theorem 2.5]), and the second condition is required by the resonance theory below. Natural choices of η for complex k that reduce to the common choice of $\eta = k$ when k is real are $\eta = k$ and $\eta = \operatorname{Re}\{k\}$; however, the latter does not satisfy the second condition above.

In a neighborhood of the real axis the resonances of the exterior scattering problem are equal to the wavenumbers k_{res} , $\operatorname{Im}\{k_{res}\} < 0$, for which $A_{k_{res},\eta}$ is not invertible (see Remark 5.2). Since $A_{k_{res},\eta}$ is Fredholm with index 0, it holds that there exists $v \in L^2(\Gamma)$, such that

$$(5.1) \quad A_{k_{res},\eta} v = 0.$$

It follows immediately that directly at a resonance k_{res} the operator $A_{k_{res},\eta}$ is not coercive. Ideally we would like to prove that around every resonance k_{res} there is a neighborhood where $A_{k,\eta}$ is not coercive. If 0 is in the interior of the numerical range of $A_{k_{res},\eta}$, then this result follows by continuity. However, it is possible that 0 might be on the boundary of the numerical range at k_{res} . The following theorem gives a sufficient condition for 0 to be in the interior of the numerical range of $A_{k_{res},\eta}$.

THEOREM 5.1. *Let $k_{res} \in \mathbb{C}$, $\text{Re}\{k_{res}\} > 0$, $\text{Im}\{k_{res}\} < 0$, be a resonance and assume that there exists $v \in L^2(\Gamma)$, such that $A_{k_{res},\eta}^* v \neq 0$, where v satisfies (5.1). Then 0 is in the interior of $W(A_{k_{res},\eta})$.*

Proof. From $A_{k_{res},\eta}^* v \neq 0$ it follows that, with $y = \frac{A_{k_{res},\eta}^* v}{\|A_{k_{res},\eta}^* v\|}$, $\langle A_{k_{res},\eta} y, v \rangle = \|A_{k_{res},\eta}^* v\| > 0$. Then for $\epsilon \in \mathbb{C}$ we have

$$\frac{\langle A_{k_{res},\eta}(v + \epsilon y), v + \epsilon y \rangle}{\langle v + \epsilon y, v + \epsilon y \rangle} = \frac{\epsilon \langle A_{k_{res},\eta} y, v \rangle + |\epsilon|^2 \langle A_{k_{res},\eta} y, y \rangle}{1 + 2\text{Re}\{\epsilon \langle y, v \rangle\} + |\epsilon|^2} =: g(\epsilon_R, \epsilon_I),$$

where $\epsilon = \epsilon_R + i\epsilon_I$. Thus, by the definition of g , $g(\alpha, \beta) \in W(A_{k_{res},\eta})$ for any $(\alpha, \beta) \in \mathbb{R}^2$ with $\alpha^2 + \beta^2$ sufficiently small. In particular $g(0, 0) = 0 \in W(A_{k_{res},\eta})$. Now define $f : \mathbb{R}^2 \rightarrow \mathbb{R}^2$ by $f(\alpha, \beta) = (\text{Re}\{g(\alpha, \beta)\}, \text{Im}\{g(\alpha, \beta)\})$. A straightforward calculation shows that

$$\det \left(\frac{\partial f(\alpha, \beta)}{\partial(\alpha, \beta)} \Big|_{\alpha=\beta=0} \right) = \|A_{k_{res},\eta}^* v\|^2 \neq 0.$$

Hence, by the inverse function theorem there exists a neighborhood $B \subset W(A_{k_{res},\eta})$ of 0, such that for every $z \in B$ there is a unique $\epsilon(z) = \epsilon_R(z) + i\epsilon_I(z) \in \mathbb{C}$ with $z = g(\epsilon_R(z), \epsilon_I(z))$. This implies that 0 is in the interior of the numerical range $W(A_{k_{res},\eta})$. \square

If $A_{k_{res},\eta}$ is a normal operator, then $A_{k_{res},\eta} v = 0$ implies $A_{k_{res},\eta}^* v = 0$ and Theorem 5.1 is not applicable since the derivative of g is not invertible. Hence, the question of whether or not Theorem 5.1 can be applied for a given domain is related to the nonnormality of the corresponding operator $A_{k_{res},\eta}$. Investigating this nonnormality is ongoing work.

In the top plot of Figure 5.12 we show a contour plot of $\log_{10}(\|A_{k,k}^{-1}\|)$ in the case of the trapping domain over a part of the negative half of the complex plane. The resonances are a subset of the poles of $A_{k,k}^{-1}$ and in [39, Proposition 7.7] it is shown that resonances are identical to the set of poles of $(I + K_k)^{-1}$ with $\text{Im}\{k\} < 0$, where K_k is the double layer potential (see Remark 5.2). For comparison we show a contour plot of $\|(I + K_k)^{-1}\|$. In this second plot the singularities on the real line are eigenvalues of the associated interior Laplace eigenvalue problem with Neumann boundary conditions.

Figure 5.13 shows a plot of the numerical range of $A_{k,k}$ for $k = 5.7 - 0.29i$, which approximately corresponds to the value of the first resonance in Figure 5.12. The numerical range clearly encloses 0. From a singular value decomposition of the discretization of $A_{k,k}$ we computed the approximate function v associated with the resonance frequency. We obtain numerically $\|A_{k,k} v\|_{L^2(\Gamma)} \approx 9.4 \cdot 10^{-3}$ and $\|A_{k,k}^* v\| \approx 3.3$, a clear indicator that the conditions of Theorem 5.1 are satisfied here.

Remark 5.2. Resonances, or scattering poles, are fundamental objects in scattering theory. A good introduction to this area is given in [39, Chap. 7], but we sketch a brief outline below. Consider the scattered field u_s for the acoustic scattering problem: this satisfies the Helmholtz equation (1.5), the radiation condition (1.7), and a Dirichlet boundary condition which we shall write as

$$u_s = f \quad \text{on } \Gamma.$$

We can then abstractly write

$$u_s = B_k f,$$

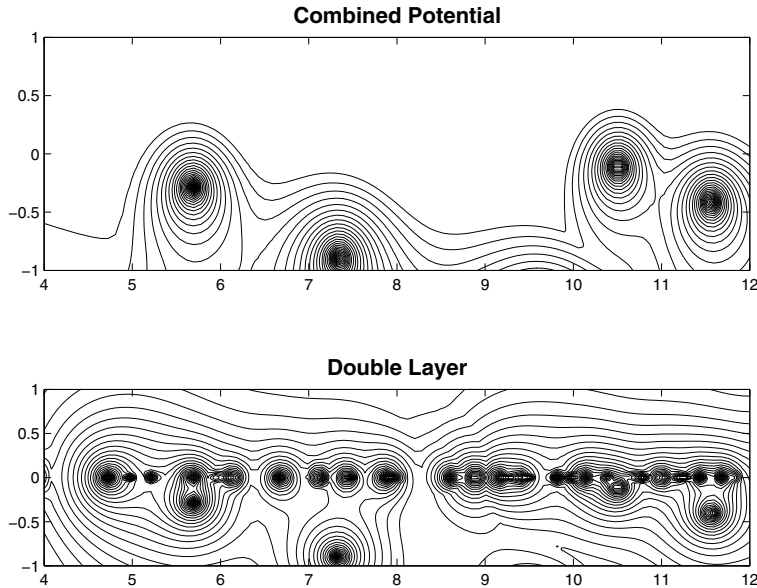


FIG. 5.12. Top: Contour plot of $\log_{10}(\|A_{k,k}^{-1}\|)$ over a part of the complex plane. Bottom: Contour plot of $\log_{10} \|(I + K_k)^{-1}\|$. In this second plot the singularities in the negative half of the complex plane are resonances, and the singularities on the real axis correspond to eigenfrequencies of the interior Neumann eigenvalue problem.

where B_k is the solution operator, and where the subscript emphasises the k -dependence. B_k is a uniquely defined operator-valued function of k for $\text{Im}\{k\} \geq 0$, and analytic for $\text{Im}\{k\} > 0$. In fact, B_k can be analytically continued into $\text{Im}\{k\} < 0$ except for certain poles, and these are called the *resonances* or *scattering poles* (in 2-d we exclude a branch cut from zero to infinity due to the logarithmic singularity of the fundamental solution at $k = 0$). When k is one of these scattering poles, there exists an outgoing solution of (1.5) which is zero on Γ , where a function v is called outgoing if

$$v \sim C \frac{e^{ikr}}{r^{(d-1)/2}} \text{ as } r \rightarrow \infty,$$

where C depends only on the angular variables and d is the dimension [27, Chap. 4, Thm. 4.3]. However, outgoing solutions with k having negative imaginary part grow exponentially towards infinity and do not satisfy the Sommerfeld radiation condition (1.7).

In a neighborhood of the positive real k axis, B_k can be expressed in terms of the boundary integral operator $A'_{k,\eta}$, (2.1), as follows:

$$(5.2) \quad B_k = 2(\mathcal{K}_k - i\eta\mathcal{S}_k)(A'_{k,\eta})^{-1},$$

where the double- and single-layer potentials are defined by

$$\mathcal{K}_k u(x) := \int_{\Gamma} \frac{\partial \Phi(x,y)}{\partial n(y)} u(y) ds(y), \quad \mathcal{S}_k u(x) := \int_{\Gamma} \Phi(x,y) u(y) ds(y), \quad x \in \mathbb{R}^d \setminus \Gamma,$$

η is an analytic function of k with $\text{Re}\{\eta\bar{k}\} > 0$ (such as $\eta = k$ or η a positive real constant), and the subscripts again emphasise the k -dependence [39, eq. (7.32)]. (The

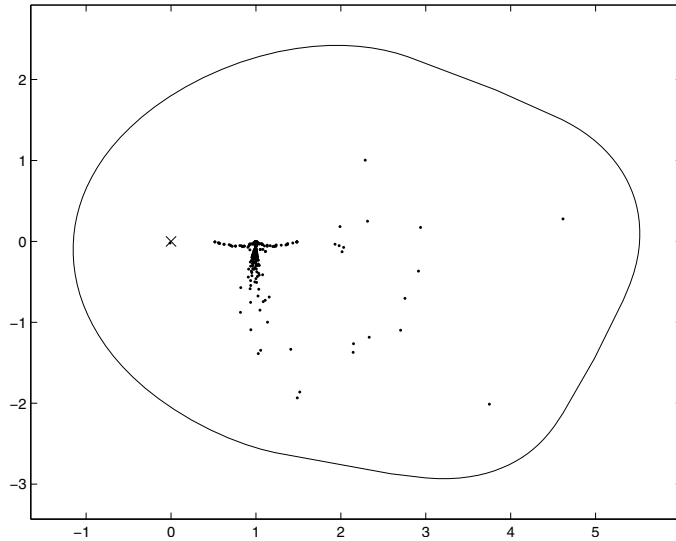


FIG. 5.13. Plot of the numerical range of $A_{k,k}$ for the trapping domain, where $k = 5.7 - 0.29i$ is the approximate value of the first resonance.

theory in [39] is for smooth domains, where $A_{k,\eta}$ is a compact perturbation of the identity. However, it also holds in the Lipschitz case because $A_{k,\eta}$ is Fredholm with index 0.) This representation of B_k shows that, in the neighborhood of \mathbb{R}^+ , where this formula is valid, the scattering poles are equal to the poles of $(A'_{k,\eta})^{-1}$, and hence to the poles of $A_{k,\eta}^{-1}$, using the fact that $\|(A'_{k,\eta})^{-1}\| = \|A_{k,\eta}^{-1}\|$ [14]. Note that the poles of $(A'_{k,\eta})^{-1}$ are independent of the particular choice of η since they are poles of both $(I + K_k)^{-1}$ and S_k^{-1} . The scattering poles, as defined above, are also equal to the poles of the so-called *scattering operators* for both the acoustic scattering problem and the time-dependent wave equation [39, Chap. 7].

6. Conclusions. Proving coercivity is still a largely open problem for the standard boundary integral formulations of acoustic scattering problems. In this paper we used the close connection to the numerical range of the operator to investigate coercivity on several interesting domains in 2-d. The numerical results demonstrate that coercivity of the direct combined boundary integral operator A seems to hold uniformly on a wide range of domains. This is surprising since for standard domain based variational formulations of the underlying Helmholtz equation only a weaker Gårding inequality, with a k -dependent perturbation term, holds [23]. Table 6.1 summarizes the results for the different domains. Coercivity seems to hold uniformly (with respect to the numerical accuracy of the results) and independently of the wavenumber for all considered domains apart from the inverted ellipse and the trapping domain. For the inverted ellipse it is not clear from the current results whether $\gamma \rightarrow 0$ as $k \rightarrow \infty$ or whether there exists a positive lower bound C , such that $C < \gamma$ for all sufficiently large k . The trapping domain behaves very differently from the other domains, and we saw that the boundary integral operator has resonances close to the real axis which helped to explain why it is not coercive. This leads us to make the following conjecture.

Conjecture 6.1. The combined boundary integral operator A is coercive on bounded domains for all wavenumbers k that are sufficiently far away from a res-

TABLE 6.1

Summary of the numerical results on coercivity of the operator A on various domains for $k = 10, 50, 100$.

	Smooth	Polygonal
Convex	Circle-coercive, uniform in k	Square-coercive, uniform in k Equilateral triangle-coercive, uniform in k
Nonconvex, star-shaped	Kite-coercive, uniform in k Inverted ellipse-coercive, not uniform in k	L-shaped-coercive, uniform in k
Nonstar-shaped		Double-L-coercive, uniform in k Trapping-coercivity depends on k

onance.

The fact that the trapping domain behaves so differently from the other domains considered here is not surprising. Indeed, in scattering theory for the time dependent wave equation, the geometry of the domain, and in particular whether it is trapping or not, plays a key role [27]. Recall the definition of *trapping* and *nontrapping* from the epilogue of [27]: consider all the rays starting in the exterior of Ω inside some large ball of finite radius. Continue all the rays according to the law of reflection (angle of incidence equals angle of reflection) whenever they hit $\partial\Omega$, until they finally leave the large ball. We call Ω trapping if there are arbitrary long paths or closed paths of this kind; otherwise Ω is nontrapping. (Note that there are subtleties associated with rays hitting the boundary at a tangent, and also for domains with nonsmooth boundaries.)

The connection between whether a domain is trapping or not and the location of resonances is a classic problem: in the 1967 first edition of [27], Lax and Philips conjectured that

1. for a nontrapping domain there are no resonances in a strip $\{k : -\alpha \leq \text{Im}\{k\} \leq 0\}$ for some constant $\alpha > 0$, and
2. for a trapping domain there is a sequence of resonances $\{k_j\}_{j=1}^{\infty}$ such that $\text{Im}\{k_j\} \rightarrow 0$ as $j \rightarrow \infty$.

The first statement was proved to be correct in [41, 33, 32]; however, an example of a trapping domain for which there are no resonances in a strip below the real axis was given in [24], and thus the second statement is incorrect. More details about these results can be found in, e.g., [27, Epilogue], [42]. (Note that the 2-d case is more subtle than the 3-d case due to the presence of a branch point in the solution operator at $k = 0$.)

Returning to the question of coercivity, result 1 above implies that for the inverted ellipse there are no resonances in a strip below the imaginary axis, lending support to the idea that coercivity is uniform for higher k . Combining Conjecture 6.1 with result 1 leads to the following conjecture.

Conjecture 6.2. The combined boundary integral operator A is coercive uniformly in k , for all sufficiently large wavenumbers k , for all nontrapping domains. (This obviously depends on whether the strip in result 1 causes the resonances to be sufficiently far away from the real axis.)

Note that, as mentioned in section 2, for a certain class of trapping domains (including the domain considered in section 5.3) A has already been proven not to be uniformly coercive in k ; however, much work still has to be done to establish whether these conjectures are true or not (or true in some modified forms). In particular, the connection between resonances/trapping and coercivity needs to be more closely

investigated.

Apart from investigating coercivity itself, this paper points to several other open research directions. We did not discuss the plots of the spectra in detail, but nevertheless they show some interesting features, especially for the polygonal domains where the operator is not a compact perturbation of the identity. In addition, the connection to nonnormality should be investigated further: it appears that the operator is non-normal for all domains other than the unit circle, and it would be interesting if this could be proved. It seems that coercivity is intimately linked to this nonnormality: indeed, as the example of the trapping domain shows, spectral information appears to be largely irrelevant for answering the question of whether coercivity holds or not. However, the behavior of nonnormal matrices and operators is still an open problem in many applications (see the book by Trefethen and Embree [40]).

Finally, with this paper we would like to advertise the use of the numerical range and related concepts like pseudospectra [40] for investigating the properties of boundary integral operators. Many interesting results can be expressed in terms of the numerical range such as the reformulation of C ea's lemma in Theorem 3.7, and estimates for iterative solvers [18, 19].

Acknowledgments. The authors would like to thank Ivan Graham (Bath) and Simon Chandler-Wilde (Reading) for helpful discussions that improved this paper. The first author would like to thank Ivan Graham for an invitation to Bath in November 2009, which started this paper. Both authors would also like to thank the referees for helpful remarks that improved this paper.

Note added in proof. Following the proof of coercivity for a modified operator in [37], A has recently been proved to be coercive, uniformly for sufficiently large k , on strictly convex smooth domains by the second author and Valery Smyshlyaev (University College London).

REFERENCES

- [1] S. AMINI, *On the choice of the coupling parameter in boundary integral formulations of the exterior acoustic problem*, Appl. Anal., 35 (1990), pp. 75–92.
- [2] S. AMINI, *Boundary integral solution of the exterior Helmholtz problem*, Comput. Mech., 13 (1993), pp. 2–11.
- [3] K. E. ATKINSON, *The Numerical Solution of Integral Equations of the Second Kind*, Cambridge Monogr. Appl. Comput. Math. 4, Cambridge University Press, Cambridge, UK, 1997.
- [4] L. BANJAI AND S. SAUTER, *A refined Galerkin error and stability analysis for highly indefinite variational problems*, SIAM J. Numer. Anal., 45 (2007), pp. 37–53.
- [5] T. BETCKE, S. N. CHANDLER-WILDE, I. G. GRAHAM, S. LANGDON, AND M. LINDNER, *Condition number estimates for combined potential boundary integral operators in acoustics and their boundary element discretisation*, Numer. Methods Partial Differential Equations, 27 (2011), pp. 31–69.
- [6] T. BRACONNIER AND N. J. HIGHAM, *Computing the field of values and pseudospectra using the Lanczos method with continuation*, BIT, 36 (1996), pp. 422–440.
- [7] H. BRAKHAGE AND P. WERNER, *Über das dirichletsche Aussenraumproblem für die Helmholtzsche Schwingungsgleichung*, Arch. Math., 16 (1965), pp. 325–329.
- [8] S. C. BRENNER AND L. R. SCOTT, *The Mathematical Theory of Finite Element Methods*, 2nd ed., Texts Appl. Math. 15, Springer, New York, 2002.
- [9] O. P. BRUNO AND L. A. KUNYANSKY, *Surface scattering in three dimensions: An accelerated high-order solver*, R. Soc. Lond. Proc. Math. Phys. Eng. Sci., 457 (2001), pp. 2921–2934.
- [10] J. V. BURKE AND A. GREENBAUM, *Characterizations of the polynomial numerical hull of degree k* , Linear Algebra Appl., 419 (2006), pp. 37–47.
- [11] S. N. CHANDLER-WILDE AND I. G. GRAHAM, *Boundary integral methods in high frequency scattering*, in Highly Oscillatory Problems: Computation, Theory and Applications, B.

- Engquist, T. Fokas, E. Hairer, and A. Iserles, eds., Cambridge University Press, Cambridge, UK, 2009, pp. 154–193.
- [12] S. N. CHANDLER-WILDE, I. G. GRAHAM, S. LANGDON, AND M. LINDNER, *Condition number estimates for combined potential boundary integral operators in acoustic scattering*, J. Integral Equations Appl., 21 (2009), pp. 229–279.
- [13] S. N. CHANDLER-WILDE AND S. LANGDON, *A Galerkin boundary element method for high frequency scattering by convex polygons*, SIAM J. Numer. Anal., 45 (2007), pp. 610–640.
- [14] S. N. CHANDLER-WILDE AND P. MONK, *Wave-number-explicit bounds in time-harmonic scattering*, SIAM J. Math. Anal., 39 (2008), pp. 1428–1455.
- [15] D. L. COLTON AND R. KRESS, *Integral Equation Methods in Scattering Theory*, Pure Appl. Math. (N.Y.), John Wiley & Sons, New York, 1983.
- [16] D. L. COLTON AND R. KRESS, *Inverse Acoustic and Electromagnetic Scattering Theory*, Springer-Verlag, Berlin, 1992.
- [17] V. DOMÍNGUEZ, I. G. GRAHAM, AND V. P. SMYSHLYAEV, *A hybrid numerical-asymptotic boundary integral method for high-frequency acoustic scattering*, Numer. Math., 106 (2007), pp. 471–510.
- [18] T. A. DRISCOLL, K.-C. TOH, AND L. N. TREFETHEN, *From potential theory to matrix iterations in six steps*, SIAM Rev., 40 (1998), pp. 547–578.
- [19] M. EMBREE, *How Descriptive Are GMRES Convergence Bounds?*, Technical report 99/08, Oxford University Computing Laboratory, Oxford, UK, 1999.
- [20] K. GIEBERMANN, *Schnelle Summationsverfahren zur numerischen Lösung von Integralgleichungen für Streuprobleme im R_3* , Ph.D. thesis, University of Karlsruhe, Karlsruhe, Germany, 1997.
- [21] I. G. GRAHAM, S. JOE, AND I. H. SLOAN, *Iterated Galerkin versus iterated collocation for integral equations of the second kind*, IMA J. Numer. Anal., 5 (1984), pp. 355–369.
- [22] K. E. GUSTAFSON AND D. K. M. RAO, *Numerical Range. The Field of Values of Linear Operators and Matrices*, Universitext, Springer-Verlag, New York, 1997.
- [23] F. IHLENBURG, *Finite Element Analysis of Acoustic Scattering*, Appl. Math. Sci. 132, Springer-Verlag, New York, 1998.
- [24] M. IKAWA, *On the poles of the scattering matrix for two strictly convex obstacles*, J. Math. Kyoto Univ., 23 (1983), pp. 127–194.
- [25] R. KRESS, *Minimizing the condition number of boundary integral operators in acoustic and electromagnetic scattering*, Quart. J. Mech. Appl. Math., 38 (1985), pp. 323–341.
- [26] R. KRESS AND W. T. SPASSOV, *On the condition number of boundary integral operators for the exterior Dirichlet problem for the Helmholtz equation*, Numer. Math., 42 (1983), pp. 77–95.
- [27] P. LAX AND R. PHILLIPS, *Scattering Theory*, 2nd ed., Academic Press, Boston, 1989.
- [28] R. LEIS, *Zur Dirichletschen Randwertaufgabe des Aussenraumes der Schwingungsgleichung*, Math. Z., 90 (1965), pp. 205–211.
- [29] M. LÖHNDORF AND J. MELENK, *Wavenumber-Explicit hp-BEM for High Frequency Scattering*, Technical report ASC Report 2/2010, Institute for Analysis and Scientific Computing—Vienna University of Technology, Vienna, Austria, 2010.
- [30] W. C. H. MCLEAN, *Strongly Elliptic Systems and Boundary Integral Equations*, Cambridge University Press, Cambridge, UK, 2000.
- [31] J. MELENK, *Mapping Properties of Combined Field Helmholtz Boundary Integral Operators*, Technical report ASC Report 1/2010, Institute for Analysis and Scientific Computing—Vienna University of Technology, Vienna, Austria, 2010.
- [32] R. MELROSE, *Singularities and energy decay in acoustical scattering*, Duke Math. J., 46 (1979), pp. 43–59.
- [33] C. S. MORAWETZ, J. V. RALSTON, AND W. A. STRAUSS, *Decay of solutions of the wave equation outside nontrapping obstacles*, Comm. Pure Appl. Math., 30 (1977), pp. 447–508.
- [34] J. NEČAS, *Les méthodes directes en théorie des équations elliptiques*, Massonet et Cie, Paris, 1967.
- [35] O. I. PANIČ, *On the question of the solvability of the exterior boundary-value problems for the wave equation and Maxwell's equations*, Uspehi Mat. Nauk, 20 (1965), pp. 221–226.
- [36] I. H. SLOAN AND A. SPENCE, *The Galerkin method for integral equations of the first kind with logarithmic kernel: Theory*, IMA J. Numer. Anal., 8 (1988), pp. 105–122.
- [37] E. A. SPENCE, S. N. CHANDLER-WILDE, I. G. GRAHAM, AND V. P. SMYSHLYAEV, *A new frequency-uniform coercive boundary integral equation for acoustic scattering*, Comm. Pure Appl. Math., to appear.
- [38] O. STEINBACH, *Numerical Approximation Methods for Elliptic Boundary Value Problems, Finite and Boundary Elements*, Springer, New York, 2008. Translated from the 2003 German original.

- [39] M. TAYLOR, *Partial Differential Equations. II, Qualitative Studies of Linear Equations*, Appl. Math. Sci. 116, Springer-Verlag, New York, 1996.
- [40] L. N. TREFETHEN AND M. EMBREE, *Spectra and Pseudospectra*, Princeton University Press, Princeton, NJ, 2005.
- [41] B. VAINBERG, *The short-wave asymptotic behaviour of the solutions of stationary problems, and the asymptotic behaviour as $t \rightarrow \infty$ of solutions of nonstationary problems*, Uspehi Mat. Nauk, 30 (1975), pp. 3–55.
- [42] B. VAINBERG, *Asymptotic Expansion as $t \rightarrow \infty$ of the Solutions of Exterior Boundary Value Problems for Hyperbolic Equations and Quasiclassical Approximations*, in *Partial Differential Equations V*, M. V. Fedoryuk, ed., Springer, New York, 1999, pp. 53–90.
- [43] G. VERCHOTA, *Layer potentials and regularity for the Dirichlet problem for Laplace's equation in Lipschitz domains*, J. Funct. Anal., 59 (1984), pp. 572–611.